

Numerical relativity for D dimensional axially symmetric space-times: formalism and code tests

Miguel Zilhão,^{1,*} Helvi Witek,^{2,†} Ulrich Sperhake,^{3,‡} Vitor Cardoso,^{2,4,§}
Leonardo Gualtieri,^{5,¶} Carlos Herdeiro,^{1,**} and Andrea Nerozzi^{2,††}

¹ *Centro de Física do Porto — CFP*
Departamento de Física e Astronomia

Faculdade de Ciências da Universidade do Porto — FCUP
Rua do Campo Alegre, 4169-007 Porto, Portugal

² *Centro Multidisciplinar de Astrofísica — CENTRA*
Departamento de Física, Instituto Superior Técnico — IST
Av. Rovisco Pais 1, 1049-001 Lisboa, Portugal

³ *California Institute of Technology*
Pasadena, CA 91125, USA

⁴ *Department of Physics and Astronomy, The University of Mississippi*
University, MS 38677-1848, USA

⁵ *Dipartimento di Fisica, Università di Roma “Sapienza” & Sezione*
INFN Roma1, P.A. Moro 5, 00185, Roma, Italy

(Dated: January 2010)

The numerical evolution of Einstein’s field equations in a generic background has the potential to answer a variety of important questions in physics: from applications to the gauge-gravity duality, to modelling black hole production in TeV gravity scenarios, analysis of the stability of exact solutions and tests of Cosmic Censorship. In order to investigate these questions, we extend numerical relativity to more general space-times than those investigated hitherto, by developing a framework to study the numerical evolution of D dimensional vacuum space-times with an $SO(D-2)$ isometry group for $D \geq 5$, or $SO(D-3)$ for $D \geq 6$.

Performing a dimensional reduction on a $(D-4)$ -sphere, the D dimensional vacuum Einstein equations are rewritten as a 3+1 dimensional system with source terms, and presented in the Baumgarte, Shapiro, Shibata and Nakamura (BSSN) formulation. This allows the use of existing 3+1 dimensional numerical codes with small adaptations. Brill-Lindquist initial data are constructed in D dimensions and a procedure to match them to our 3+1 dimensional evolution equations is given. We have implemented our framework by adapting the LEAN code and perform a variety of simulations of non-spinning black hole space-times. Specifically, we present a modified *moving puncture* gauge which facilitates long term stable simulations in $D = 5$. We further demonstrate the internal consistency of the code by studying convergence and comparing numerical versus analytic results in the case of geodesic slicing for $D = 5, 6$.

PACS numbers: 04.25.D-, 04.25.dg, 04.50.-h, 04.50.Gh

*Electronic address: mzilhao@fc.up.pt

†Electronic address: helvi.witek@ist.utl.pt

‡Electronic address: sperhake@tapir.caltech.edu

§Electronic address: vitor.cardoso@ist.utl.pt

¶Electronic address: leonardo.gualtieri@roma1.infn.it

**Electronic address: crherdei@fc.up.pt

††Electronic address: andrea.nerozzi@ist.utl.pt

Contents

1. Introduction	2
1.1. Motivation	3
1.2. Space-times with symmetries	4
1.3. Axial symmetry $SO(D - 2)$ and $SO(D - 3)$	5
2. The effective 3+1 dimensional system	6
2.1. $4 + (D - 4)$ split	7
2.2. Dimensional reduction on a $(D - 4)$ -sphere and $3 + 1$ split	9
2.3. BSSN formulation	11
3. Initial data	13
3.1. D dimensional Hamiltonian and momentum constraints	13
3.2. Brill-Lindquist initial data and matching to four dimensions	14
3.2.1. Evolution of a single black hole	15
3.2.2. Head-on collision of black holes	15
4. The numerical treatment	16
4.1. Numerical results in $D = 5$	16
4.2. Preliminary numerical results in $D = 6$	19
5. Final Remarks	21
Acknowledgments	21
A. Implementing regular variables	22
B. Analysis of troublesome terms at $y = 0$	24
C. Geodesic slicing	26
References	28

1. INTRODUCTION

Numerical relativity is an essential tool to study many processes involving strong gravitational fields. In four space-time dimensions, processes of this sort, such as black hole (BH) binary evolutions, are of utmost importance for understanding the main sources of gravitational waves, which are expected to be detected by the next generation of ground based [Laser Interferometer Gravitational-Wave Observatory (LIGO), VIRGO] and space based [Laser Interferometer Space Antenna (LISA)] interferometers. Long-term stable numerical evolutions of BH binaries have finally been achieved after four decades of efforts [1–3]. The numerical modelling of generic spinning BH binaries in vacuum Einstein gravity is an active field of research, with important consequences for gravitational wave detection in the near future.

Numerical relativity in a higher dimensional space-time, instead, is an essentially unexplored field, with tremendous potential to provide answers to some of the most fundamental questions in physics. Recent developments in experimental and theoretical physics make this a pressing issue. We refer, in particular, to the prominent role of BHs in the gauge-gravity duality, in TeV-scale gravity or even on their own as solutions of the field equations. These are some of the most active areas of current research in gravitational and high energy physics.

1.1. Motivation

i. AdS/CFT and holography. In 1997–98, a powerful new technique known as the AdS/CFT correspondence or, more generally, the gauge-string duality, was introduced and rapidly developed [4]. This holographic correspondence provides an effective description of a non-perturbative, strongly coupled regime of certain gauge theories in terms of higher-dimensional classical gravity. In particular, equilibrium and non-equilibrium properties of strongly coupled thermal gauge theories are related to the physics of higher-dimensional BHs, black branes and their fluctuations. These studies revealed intriguing connections between the dynamics of BH horizons and hydrodynamics [5], and offer new perspectives on notoriously difficult problems, such as the BH information loss paradox, the nature of BH singularities or quantum gravity.

Numerical relativity in anti-de Sitter backgrounds is bound to contribute enormously to our understanding of the gauge-gravity duality and is likely to have important applications in the interpretation of observations [6–9]. For instance, in the context of the gauge-gravity duality, high energy collisions of BHs have a dual description in terms of *a)* high energy collisions with balls of de-confined plasma surrounded by a confining phase and *b)* the rapid localised heating of a de-confined plasma. These are the type of events that may have direct observational consequences for the experiments at Brookhaven’s Relativistic Heavy Ion Collider (RHIC) [8, 9]. Numerical relativity in anti-de Sitter is notoriously difficult, and so far only very special situations have been handled [10, 11]. The phenomenologically most interesting case is a five dimensional space-time, AdS_5 , and therefore the higher dimensional extension of numerical relativity is necessary.

ii. TeV-scale gravity scenarios. An outstanding problem in high energy physics is the extremely large ratio between the four dimensional Planck scale, 10^{19} GeV, and the electroweak scale, 10^2 GeV. It has been proposed that this *hierarchy problem* can be resolved if one adopts the idea that the Standard Model is confined to a brane in a higher dimensional space, such that the extra dimensions are much larger than the four dimensional Planck scale (they may be large up to a sub-millimetre scale) [12–14]. In a different version of the model, the extra dimensions are infinite, but the metric has an exponential factor introducing a finite length scale [15, 16].

In such models, the fundamental Planck scale could be as low as 1 TeV. Thus, high energy colliders, such as the Large Hadron Collider (LHC), may directly probe strongly coupled gravitational physics [17–22]. In fact, such tests may even be routinely available in the collisions of ultra-high energy cosmic rays with the Earth’s atmosphere [23–25], or in astrophysical BH environments [26–28] (for reviews see [29–31]). From Thorne’s hoop conjecture it follows that, in this scenario, particle collisions could produce BHs [19, 20]. Moreover, the production of BHs at trans-Planckian collision energies (compared to the fundamental Planck scale) should be well described by using classical general relativity extended to D dimensions [18–25, 29–33]. The challenge is then to use the classical framework to determine the cross section for production and, for each initial setup, the fractions of the collision energy and angular momentum that are lost in the higher dimensional space by emission of gravitational waves. This information will be of paramount importance to improve the modelling of microscopic BH production in event generators such as TRUENOIR, CHARYBDIS2, CATFISH or BLACKMAX [20, 34–37]. The event generators will then provide a description of the corresponding evaporation phase, which might be observed during LHC collisions.

The first models for BH production in parton-parton collisions used a simple black disk approach to estimate the cross section for production [19, 20]. Improved bounds have

been obtained using either trapped surface methods to estimate the cross section for BH production [38–41] or approximation schemes [42–47] to evaluate the gravitational energy loss. Only recently exact results for highly relativistic collisions were obtained in four dimensions, using numerical relativity techniques [48–50]. No such exact results are yet available in the higher dimensional case. To obtain them is one of our main goals and the present paper introduces a formalism to achieve that.

iii. Higher dimensional black holes. Asymptotically flat higher dimensional black objects have a much richer structure than their four dimensional counterparts. For instance, spherical topology is not the only allowed topology for objects with a horizon. One can also have, *e.g.*, black rings, with a donut-like topology. Remarkably, these two different horizon topologies coexist for certain regions in phase-space [51]. The stability of general higher-dimensional BHs is now starting to be explored. Generically it has been conjectured that for $D \geq 6$ ultra-spinning Myers-Perry BHs will be unstable [52]. This instability has been confirmed by an analysis of linearised axi-symmetric perturbations in $D = 7, 8, 9$ [53]. Clearly, the study of the non-linear development of these instabilities requires numerical methods, such as the ones presented herein. A study of this type was very recently presented for a non axi-symmetric perturbation in $D = 5$ [54], where it was found that a single spinning five dimensional Myers-Perry BH is unstable, for sufficiently large rotation parameter (thereby confirming previous conjectures [55–57]).

Not much is known about general equilibrium states in anti-de Sitter backgrounds. The gauge-gravity duality and the hydrodynamic limit have been used to predict the existence of larger classes of BHs in anti-de Sitter backgrounds, including non axi-symmetric solutions [56, 57]. However, these have not yet been found.

Finally, there are issues of principle, as for example testing Cosmic Censorship in BH collisions [48, 50] which require state-of-the-art numerical simulations.

1.2. Space-times with symmetries

From what has been said, the extension of four dimensional numerical Relativity is mandatory. Some pioneering works have been concerned with the non-linear development of the Gregory-Laflamme instability [58] of cosmic strings [59] and gravitational collapse, with spherical symmetry [60], axial symmetry [61] or even static situations [62]. Another numerical code, based on the cartoon method [63], was developed and tested for five space-time dimensions in Ref. [64]. See also Ref. [65] for a discussion of slicings of D dimensional black holes. The (phenomenologically) most interesting large extra dimensions models are, however, in higher than five space-time dimensions (see for instance [30]). Moreover, the ultra-spinning instabilities of Myers-Perry BHs should occur in $D \geq 6$. Thus, our approach here is to develop a framework and a numerical code that can, in principle, be applied to different space-time dimensions with little adaptations. This may be achieved by taking the D dimensional vacuum space-time to have an isometry group fit to include a large class of interesting problems. If this isometry group is sufficiently large, it allows a dimensional reduction of the problem to 3+1 dimensions, wherein it appears as (four dimensional) general relativity coupled to some *quasi-matter* terms.¹ Thus, the different space-time dimension manifests itself only in the different quasi-matter content of the four dimensional

¹ Hereafter, we dub the source terms of the lower dimensional Einstein equations as *quasi-matter*, since its energy-momentum tensor is not that of canonical matter.

theory. We emphasise, in this context, that full blown $4 + 1$, $5 + 1$, *etc.* numerical simulations without symmetry are currently not possible due to the computational costs, so that our approach pushes numerical relativity in higher dimensions to the outmost practical limits of the present time. Moreover, an obvious advantage of this approach is that we can use existing codes with small adaptations: the four dimensional equations need to be coupled to the appropriate quasi-matter terms and some issues related to the chosen coordinates must be addressed, as we shall see. Finally, the lessons learnt in treating our effective gravity plus quasi-matter system might be of use in dealing with other four dimensional numerical relativity problems with sources.

1.3. Axial symmetry $SO(D - 2)$ and $SO(D - 3)$

We consider two classes of models, which are generalisations of axial symmetry to higher dimensional space-times: a $D \geq 5$ dimensional vacuum space-time with an $SO(D - 2)$ isometry group, and a $D \geq 6$ dimensional vacuum space-time with an $SO(D - 3)$ isometry group. The former class allows studies of head-on collisions of non-spinning BHs. In order to end up with a $3 + 1$ dimensional model we use, however, only part of this symmetry: we perform a dimensional reduction by isometry on a $(D - 4)$ -sphere which has an $SO(D - 3) \subset SO(D - 2)$ isometry group. The latter class allows to model BH collisions with impact parameter and with spinning BHs, as long as all the dynamics take place on a single plane.² In this case we perform a dimensional reduction by isometry on the entire $SO(D - 3)$ isometry group. This class includes the most interesting physical configurations relevant to accelerator—and cosmic ray—physics (in the context of TeV-scale gravity), and to the theoretical properties of higher-dimensional black objects (such as stability and phase diagrams).

We formulate the evolution equations in the Baumgarte, Shapiro, Shibata and Nakamura (BSSN) formulation [66, 67], together with the moving puncture approach [2, 3]. This is known to provide a stable evolution scheme for vacuum solutions in four dimensions, and therefore it is the natural framework for our Einstein plus quasi-matter system. The quasi-matter terms however, exhibit a problem for numerical evolution, well known from other numerical studies using coordinates adapted to axial symmetry, which is sourced by the existence of a coordinate singularity at the axis. In our formulation, this problem appears when a certain 3+1 dimensional Cartesian coordinate vanishes, $y = 0$. We present a detailed treatment of this problem, introducing first regular variables, then analysing one by one all potentially pathological terms in our evolution equations and finally presenting a method to heal all of them. The resulting equations have no further (obvious) problems for numerical evolution and could, in principle, be implemented in any working 3+1 dimensional numerical relativity code.

Here we present numerical results using the LEAN code [68], developed by one of us. We stress that the formalism developed here is valid in general D . However, long term stable evolutions typically require some experiments with free parameters in the gauge conditions and also possibly with constraint damping. For $D = 5$ we show that, if appropriate gauge conditions are chosen, the numerical evolution for Brill-Lindquist initial data describing a single BH is stable and the constraints are preserved in the evolution, within numerical error. As another test, we evolve the same initial data in a geodesic slicing gauge. This gauge is inappropriate for a long term evolution; but it allows us to compare the numerical evolution with the analytic solution for a single Tangherlini BH in $D = 5$. We find excellent agreement between the two. We also present some preliminary results for $D = 6$.

² This follows from the fact that the angular momenta of the black holes are parallel to the orbital angular momentum.

This paper is organised as follows. In Section 2, we discuss the D dimensional ansatz, perform the dimensional reduction by isometry, perform the Arnowitt-Deser-Misner (ADM) split and present the BSSN formulation of our equations. In Section 3, the construction of Brill-Lindquist initial data in D dimensions is discussed and a procedure to match it to our $3 + 1$ formulation is given. In Section 4 we present the numerical treatment and results. We draw our conclusions and discuss implications of our results for future work in Section 5. A considerable part of the technical details for the numerical treatment is organised into three appendices. In Appendix A we motivate and discuss the introduction of regular variables at $y = 0$ and present all relevant equations in terms of these variables. In Appendix B we explain how to tackle all the problematic terms at $y = 0$ in these equations. Finally, in Appendix C, we discuss the construction of the geodesic slicing which is used to compare analytical with numerical results.

2. THE EFFECTIVE 3+1 DIMENSIONAL SYSTEM

The starting point of the formalism used here is a dimensional reduction from D dimensional general relativity in vacuum to a four dimensional model. The isometry group of D dimensional Minkowski space-time is $ISO(1, D - 1)$; solutions of general relativity (or of other metric theories of gravity) generically break this symmetry into a subgroup. For instance, the isometry group of a Schwarzschild (or, for $D > 4$, Tangherlini [69]) BH is $SO(D - 1) \times \mathbb{R}$, whereas for a head-on collision of two non-rotating BHs it is $SO(D - 2)$: indeed, neither the time direction nor the direction of the collision correspond to symmetries, but a rotation of the remaining $D - 2$ spatial directions leaves the space-time invariant. The total space-time can then be considered as the semi-direct product of a three dimensional space-time \mathcal{N} with the sphere $S^{D-3} = SO(D - 2)/SO(D - 3)$. A coordinate system for \mathcal{N} can be given, for example in the case of a head-on collision of two BHs, by the time t , the coordinate z along the collision axis, and the distance from that axis.

One can take advantage of this symmetry to reduce the space-time dimensionality. This can be accomplished by writing Einstein's equations in D dimensions in a coordinate system which makes the symmetry manifest, allowing for a lower dimensional interpretation of the D dimensional Einstein's equations (in the spirit of Kaluza-Klein reduction). We remark, however, that we are not performing a compactification; rather, we perform a dimensional reduction by isometry, as first proposed by Geroch [70]. The extra dimensions manifest themselves in the lower dimensionality as a source of Einstein's equations, defined on the lower dimensional manifold.

In principle, one could use the symmetry in a more naïve way, assuming that the solution does not depend on the coordinates parameterizing the sphere and simply evolving the relevant components of the D dimensional Einstein's equations. The perspective provided by dimensional reduction, however, has two advantages: (i) all quantities have a geometrical interpretation, and this allows for a deeper understanding of the problem and a better control of the equations; (ii) it is possible to use, with minor modifications, the numerical codes which have already been written to implement Einstein's equations in a four dimensional space-time. Therefore, we do not use the entire $SO(D - 2)$ symmetry of the process, but only a $SO(D - 3)$ subgroup. This reduces the space-time on a $(D - 4)$ -sphere and yields a four dimensional manifold.

In the original proposal of Geroch [70] the symmetry space was $SO(2)$. This approach has been applied to numerical relativity, see for instance [71–73]; a five dimensional extension, with the same symmetry space, has been derived in [74]. A generalisation to coset manifolds (like the sphere S^n) was given by Cho in [75, 76], but in these papers the complete form of Einstein's equations was not presented. Here we provide the explicit form of Einstein's equations for symmetry spaces S^n together with their numerical implementation.

2.1. $4 + (D - 4)$ split

We now describe in detail the reduction from D to 4 dimensions. In order to highlight the particular classes of BH binaries we are able to study with this framework, it is convenient to begin this discussion with the isometry group of the S^{D-3} sphere, i. e. with the $3 + (D - 3)$ split.

A general D dimensional space-time metric may be written in the form

$$d\hat{s}^2 = \hat{g}_{MN} dx^M dx^N = g_{\bar{\mu}\bar{\nu}}(x^M) dx^{\bar{\mu}} dx^{\bar{\nu}} + \Omega_{\bar{i}\bar{j}}(x^M) \left(dx^{\bar{i}} - A_{\bar{\mu}}^{\bar{i}}(x^M) dx^{\bar{\mu}} \right) \left(dx^{\bar{j}} - A_{\bar{\nu}}^{\bar{j}}(x^M) dx^{\bar{\nu}} \right), \quad (2.1)$$

where we have split the space-time coordinates as $x^M = (x^{\bar{\mu}}, x^{\bar{i}})$; $M, N = 0, \dots, D - 1$ are space-time indices, $\bar{\mu}, \bar{\nu} = 0, 1, 2$ are three dimensional indices and $\bar{i}, \bar{j} = 3, \dots, D - 1$ are indices in the remaining $D - 3$ dimensions. We may think of the space-time as a fibre bundle; $\{x^{\bar{i}}\}$ are coordinates along the fibre and $\{x^{\bar{\mu}}\}$ are coordinates on the base space.

We are interested in studying D dimensional space-times with an $SO(D - 2)$ isometry group. This is the isometry group of the S^{D-3} sphere, which justifies why we are performing a $3 + (D - 3)$ splitting of the D dimensional space-time. Thus, we assume that ξ_a , $a = 1, \dots, (D - 3)(D - 2)/2$, are Killing vector fields,

$$\mathcal{L}_{\xi_a} \hat{g}_{MN} = 0, \quad (2.2)$$

with Lie algebra

$$[\xi_a, \xi_b] = \epsilon_{ab}{}^c \xi_c, \quad (2.3)$$

where $\epsilon_{ab}{}^c$ are the structure constants of $SO(D - 2)$. Because the fibre has the minimal dimension necessary to accommodate $(D - 3)(D - 2)/2$ independent Killing vector fields, we may assume without loss of generality that the Killing vector fields have components exclusively along the fibre: $\xi_a = \xi_a^{\bar{i}} \partial_{\bar{i}}$. Furthermore, we may normalise the Killing vectors so that they only depend on the coordinates of the fibre, i. e. $\partial_{\bar{\mu}} \xi_a^{\bar{i}} = 0$. Then Eq. (2.2) gives the following conditions

$$\mathcal{L}_{\xi_a} \Omega_{\bar{i}\bar{j}} = 0, \quad (2.4)$$

$$\mathcal{L}_{\xi_a} A_{\bar{\mu}}^{\bar{i}} = 0, \quad (2.5)$$

$$\mathcal{L}_{\xi_a} g_{\bar{\mu}\bar{\nu}} = 0. \quad (2.6)$$

These expressions can be interpreted either as Lie derivatives of rank-2 tensors defined on the D dimensional space-time, or as Lie derivatives of a rank-2 tensor, a vector and a scalar, which are defined on S^{D-3} .

Conditions (2.4)-(2.6) have the following implications:

$$\Omega_{\bar{i}\bar{j}} = f(x^{\bar{\mu}}) h_{\bar{i}\bar{j}}^{S^{D-3}}, \quad (2.7)$$

because, from (2.4), $\Omega_{\bar{i}\bar{j}}$ admits the maximal number of Killing vector fields and thus must be the metric on a maximally symmetric space at each $x^{\bar{\mu}}$. Due to (2.3) this space must be the S^{D-3} sphere. $h_{\bar{i}\bar{j}}^{S^{D-3}}$ denotes the metric on an S^{D-3} with unit radius;

$$g_{\bar{\mu}\bar{\nu}} = g_{\bar{\mu}\bar{\nu}}(x^{\bar{\mu}}), \quad (2.8)$$

because the Killing vector fields ξ_a act transitively on the fibre and therefore the base space metric must be independent of the fibre coordinates;

$$A_{\bar{\mu}}^{\bar{i}} = 0, \quad (2.9)$$

because Eq. (2.5) is equivalent to

$$[\xi_a, A_{\bar{\mu}}] = 0, \quad (2.10)$$

and there exist no non-trivial vector fields on S^{D-3} for $D \geq 5$ that commute with all Killing vector fields on the sphere.

We remark that (2.10) corresponds to the statement, expressed in [75] in group theoretical language, that the gauge group for a theory reduced on a coset space G/H is the normaliser of H in G ; in the case of a sphere, where $G = SO(D-2)$ and $H = SO(D-3)$, the normaliser vanishes and then there are no ‘‘gauge vectors’’, *i.e.*, no non-vanishing metric components $g_{\bar{\mu}\bar{i}}$. If the normaliser of H in G is non-vanishing, such metric components appear, and with dimensional reduction they yield vector fields which contribute to the stress-energy tensor in the reduced theory. For example, in the case of head-on collision, if $D = 4$, the isometry space is $SO(2)$ and the quasi-matter of the reduced theory consists of a scalar field and of a vector field (as in [70] and in [71–73]); if $D > 4$, the isometry space is $SO(D-2)/SO(D-3)$, and the quasi-matter of the reduced theory consists of a single scalar field. In the remainder of this work we focus on this subclass of space-times, which already contains a vast class of physically relevant problems, and postpone a discussion of the general case with $A_{\bar{\mu}}^{\bar{i}} \neq 0$ (*i.e.*, with $g_{\bar{\mu}\bar{i}} \neq 0$) to future work.

In practice, we are actually interested in performing a $4 + (D-4)$ split of the D dimensional space-time. This may be done as follows. The metric on a unit S^{D-3} may always be written in terms of the line element on a unit S^{D-4} , denoted by $d\Omega_{D-4}$, as follows,

$$h_{\bar{i}\bar{j}}^{S^{D-3}} dx^{\bar{i}} dx^{\bar{j}} = d\theta^2 + \sin^2 \theta d\Omega_{D-4}, \quad (2.11)$$

where θ is a polar-like coordinate, $\theta \in [0, \pi]$. Now we introduce four dimensional coordinates, $x^\mu = (x^{\bar{\mu}}, \theta)$, $\mu = 0, 1, 2, 3$, and define a four dimensional metric

$$g_{\mu\nu} dx^\mu dx^\nu = g_{\bar{\mu}\bar{\nu}} dx^{\bar{\mu}} dx^{\bar{\nu}} + f(x^{\bar{\mu}}) d\theta^2, \quad (2.12)$$

as well as a new conformal factor

$$\lambda(x^\mu) = \sin^2 \theta g_{\theta\theta}. \quad (2.13)$$

Then, the most general D dimensional metric compatible with $SO(D-2)$ isometry is, for $D \geq 5$

$$d\hat{s}^2 = g_{\mu\nu} dx^\mu dx^\nu + \lambda(x^\mu) d\Omega_{D-4}. \quad (2.14)$$

Without specifying (2.12) and (2.13), the geometry (2.14) has only a manifest $SO(D-3)$ symmetry. We now perform a dimensional reduction on a $(D-4)$ -sphere. This yields, from the D dimensional vacuum Einstein equations, a set of $3+1$ dimensional Einstein equations coupled to quasi-matter. If $SO(D-2)$ is the full isometry group, the quasi-matter terms do not contain independent degrees of freedom; rather, they may be completely determined by the $3+1$ dimensional geometry, via (2.13). In this case, we could perform a dimensional reduction on a $(D-3)$ -sphere, which has the full isometry group $SO(D-2)$. This would yield a $2+1$ dimensional system. The former method allows, however, the use of existing numerical codes, with small changes, which justifies our choice.

The equations derived with dimensional reduction on a $(D-4)$ -sphere can be applied, of course, to describe also space-times in which the *full* isometry group is $SO(D-3)$. This is the isometry group of a class of BH collisions with impact parameter and with spin: the collisions in

which the two BHs always move on the same 2-plane and the only non trivial components of the spin 2-form are on that same 2-plane – see Fig. 1. With our framework we are able, therefore, to describe not only head-on collisions of spinless BHs but also a class of collisions for spinning BHs with impact parameter. As follows from the discussion of (2.9), the ansatz (2.14) describes general space-times with $SO(D-3)$ isometry in $D \geq 6$. We remark that the models with $D \geq 6$ are actually the most interesting for phenomenological studies of large extra dimensions models (see for instance [30]).

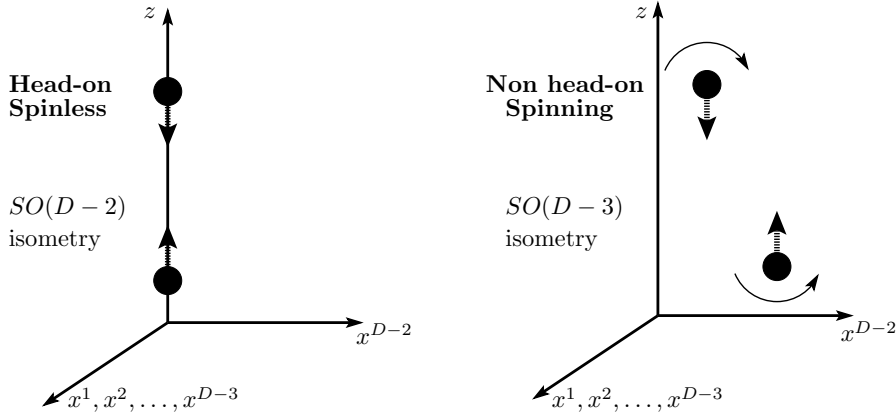


FIG. 1: D dimensional representation, using coordinates $(t, x^1, x^2, \dots, x^{D-3}, x^{D-2}, z)$, of two types of BH collisions: (left panel) head-on for spinless BHs, for which the isometry group is $SO(D-2)$; (right panel) non head-on, with motion on a *single* 2-plane, for BHs spinning in that *same* plane only, for which the isometry group is $SO(D-3)$. The figures make manifest the isometry group in both cases.

2.2. Dimensional reduction on a $(D-4)$ -sphere and 3 + 1 split

In the following we take (2.14) as an ansatz, which has a manifest $SO(D-3)$ isometry. The D dimensional pure Einstein theory reduces then to a four dimensional theory of gravity coupled to a scalar field $\lambda(x^\mu)$. We remark that in this theory λ and $g_{\mu\nu}$ are viewed as independent degrees of freedom; the relations (2.12), (2.13) select a subset of the solution space. The solutions belonging to this subset have enhanced isometry $SO(D-2)$ and correspond to some of the physical processes we want to study (for instance, head-on collisions of spinless BHs).

The D dimensional Einstein-Hilbert action reduces to

$$\mathcal{S} = \frac{1}{16\pi G_4} \int d^4x \sqrt{-g} \lambda^{\frac{D-4}{2}} \left[R + (D-4) \left((D-5)\lambda^{-1} - \lambda^{-1} \square \lambda - \frac{D-7}{4} \lambda^{-2} \partial_\mu \lambda \partial^\mu \lambda \right) \right], \quad (2.15)$$

where the D dimensional Newton's constant G_D is related to the four dimensional one G_4 by the area of the unit $D-4$ dimensional sphere: $G_4 = G_D / A^{S^{D-4}}$. Explicitly, the D dimensional Einstein's equations in vacuum yield the following system of four dimensional equations coupled to a scalar field:

$$R_{\mu\nu} = \frac{D-4}{2\lambda} \left(\nabla_\mu \partial_\nu \lambda - \frac{1}{2\lambda} \partial_\mu \lambda \partial_\nu \lambda \right), \quad (2.16)$$

$$\nabla^\mu \partial_\mu \lambda = 2(D-5) - \frac{D-6}{2\lambda} \partial_\mu \lambda \partial^\mu \lambda. \quad (2.17)$$

In these equations, all operators are covariant with respect to the four dimensional metric $g_{\mu\nu}$. The energy momentum tensor is³

$$T_{\mu\nu} = \frac{D-4}{16\pi\lambda} \left[\nabla_\mu \partial_\nu \lambda - \frac{1}{2\lambda} \partial_\mu \lambda \partial_\nu \lambda - (D-5)g_{\mu\nu} + \frac{D-5}{4\lambda} g_{\mu\nu} \partial_\alpha \lambda \partial^\alpha \lambda \right]. \quad (2.18)$$

With this four dimensional perspective, the usual 3 + 1 split of space-time [77, 78] can be performed (see, *e.g.* [79, 80]). For this purpose, we introduce the projection operator $\gamma_{\mu\nu}$ and the normal to the three dimensional hyper-surface Σ , n^μ ($n^\mu n_\mu = -1$),

$$\gamma_{\mu\nu} = g_{\mu\nu} + n_\mu n_\nu, \quad (2.19)$$

as well as the lapse α and shift β^μ ,

$$\partial_t = \alpha n + \beta, \quad (2.20)$$

where t is the time coordinate. The four dimensional metric is then written in the form

$$ds^2 = g_{\mu\nu} dx^\mu dx^\nu = -\alpha^2 dt^2 + \gamma_{ij} (dx^i + \beta^i dt)(dx^j + \beta^j dt), \quad i, j = 1, 2, 3. \quad (2.21)$$

As usual, we introduce the extrinsic curvature $K_{ij} = -\frac{1}{2}\mathcal{L}_n \gamma_{ij}$, which gives the evolution equation for the 3-metric,

$$(\partial_t - \mathcal{L}_\beta) \gamma_{ij} = -2\alpha K_{ij}. \quad (2.22)$$

The time evolution for K_{ij} is given by

$$(\partial_t - \mathcal{L}_\beta) K_{ij} = -D_i \partial_j \alpha + \alpha \left({}^{(3)}R_{ij} + K K_{ij} - 2K_{ik} K^k_j \right) - \alpha \gamma^\mu_i \gamma^\nu_j R_{\mu\nu}, \quad (2.23)$$

where D_i is the covariant derivative on the hyper-surface. The last term, $\gamma^\mu_i \gamma^\nu_j R_{\mu\nu}$, vanishes for vacuum solutions. In the present case, it is given by the projection of equation (2.16),

$$\gamma^\mu_i \gamma^\nu_j R_{\mu\nu} = \frac{D-4}{2\lambda} \left(\gamma^\mu_i \gamma^\nu_j \nabla_\mu \partial_\nu \lambda - \frac{1}{2\lambda} \partial_i \lambda \partial_j \lambda \right). \quad (2.24)$$

Using the formula

$$D_\alpha D_\beta \lambda = -K_{\alpha\beta} n^\sigma \partial_\sigma \lambda + \gamma^\mu_\alpha \gamma^\nu_\beta \nabla_\nu \partial_\mu \lambda, \quad (2.25)$$

and defining the variable

$$K_\lambda \equiv -\frac{1}{2}\mathcal{L}_n \lambda = -\frac{1}{2}n^\mu \partial_\mu \lambda, \quad (2.26)$$

we obtain

$$\gamma^\mu_i \gamma^\nu_j \nabla_\nu \partial_\mu \lambda = D_i \partial_j \lambda - 2K_{ij} K_\lambda. \quad (2.27)$$

Thus, (2.23) becomes

$$\begin{aligned} (\partial_t - \mathcal{L}_\beta) K_{ij} &= -D_i \partial_j \alpha + \alpha \left({}^{(3)}R_{ij} + K K_{ij} - 2K_{ik} K^k_j \right) \\ &\quad - \alpha \frac{D-4}{2\lambda} \left(D_i \partial_j \lambda - 2K_{ij} K_\lambda - \frac{1}{2\lambda} \partial_i \lambda \partial_j \lambda \right). \end{aligned} \quad (2.28)$$

³ We use the standard form of the Einstein equations $G_{\mu\nu} = 8\pi T_{\mu\nu}$ and choose geometrised units throughout.

To summarise, the evolution equations for the 3-metric and extrinsic curvature are (2.22) and (2.28).

If the isometry group is $SO(D-3)$, the quasi-matter field λ represents an independent degree of freedom, and we need to solve the evolution equations for λ and K_λ . Even in the case of the larger isometry $SO(D-2)$, the evolution equations for λ and K_λ are useful as they enable us to test Eq. (2.13) and thus provide a check of the numerical evolution. The evolution equation for λ is (2.26)

$$(\partial_t - \mathcal{L}_\beta)\lambda = -2\alpha K_\lambda. \quad (2.29)$$

Eq. (2.17) provides an evolution equation for K_λ . The contraction of Eq. (2.25) with $g^{\alpha\beta}$, yields

$$\square\lambda = \gamma^{ij}D_i\partial_j\lambda - 2KK_\lambda - n^\mu n^\nu \nabla_\nu \partial_\mu \lambda. \quad (2.30)$$

Noting that

$$\mathcal{L}_n K_\lambda = n^\mu \partial_\mu K_\lambda = -\frac{1}{2}n^\mu \nabla_\mu n^\nu \partial_\nu \lambda - \frac{1}{2}n^\mu n^\nu \nabla_\mu \partial_\nu \lambda, \quad (2.31)$$

and

$$n^\mu \nabla_\mu n^\nu = \frac{1}{\alpha} D^\nu \alpha, \quad (2.32)$$

we obtain

$$-n^\mu n^\nu \nabla_\mu \partial_\nu \lambda = 2\mathcal{L}_n K_\lambda + \frac{1}{\alpha} D^\nu \alpha \partial_\nu \lambda. \quad (2.33)$$

Noticing also that $D^\nu \alpha \partial_\nu \lambda = \gamma^{ij} \partial_i \alpha \partial_j \lambda$, we write

$$\square\lambda = \gamma^{ij}D_i\partial_j\lambda - 2KK_\lambda + 2\mathcal{L}_n K_\lambda + \frac{1}{\alpha}\gamma^{ij}\partial_i\alpha\partial_j\lambda. \quad (2.34)$$

Moreover, from equation

$$D_\mu \lambda = \gamma^\nu{}_\mu \partial_\nu \lambda = \partial_\mu \lambda - 2n_\mu K_\lambda, \quad (2.35)$$

we get

$$\partial_\alpha \lambda \partial^\alpha \lambda = \gamma^{ij} \partial_i \lambda \partial_j \lambda - 4K_\lambda^2, \quad (2.36)$$

so that the evolution equation for K_λ is

$$\frac{1}{\alpha}(\partial_t - \mathcal{L}_\beta)K_\lambda = -\frac{1}{2\alpha}\gamma^{ij}\partial_i\lambda\partial_j\alpha + (D-5) + KK_\lambda + \frac{D-6}{\lambda}K_\lambda^2 - \frac{D-6}{4\lambda}\gamma^{ij}\partial_i\lambda\partial_j\lambda - \frac{1}{2}D^k\partial_k\lambda. \quad (2.37)$$

Equations (2.29) and (2.37) are the evolution equations for the quasi-matter degrees of freedom.

2.3. BSSN formulation

For numerical implementation, let us now write the evolution equations in the Baumgarte, Shapiro, Shibata and Nakamura (BSSN) formulation [66, 67]. Instead of evolving the variables γ_{ij} and K_{ij} , we introduce a conformal split of the physical 3-metric γ_{ij} as

$$\gamma_{ij} \equiv \frac{1}{\chi} \tilde{\gamma}_{ij}. \quad (2.38)$$

The conformal factor

$$\chi = (\det \gamma_{ij})^{-1/3}, \quad (2.39)$$

is chosen such that $\det \tilde{\gamma}_{ij} = 1$ holds at all times. The extrinsic curvature is split into a conformal traceless part, \tilde{A}_{ij} , and its trace, K , as

$$\tilde{A}_{ij} \equiv \chi \left(K_{ij} - \frac{\gamma_{ij}}{3} K \right). \quad (2.40)$$

Moreover, we introduce the contracted conformal connection

$$\tilde{\Gamma}^i = \tilde{\gamma}^{jk} \tilde{\Gamma}_{jk}^i, \quad (2.41)$$

where

$$\Gamma_{ij}^k = \tilde{\Gamma}_{ij}^k - \frac{1}{2\chi} (\delta_i^k \partial_j \chi + \delta_j^k \partial_i \chi - \tilde{\gamma}_{ij} \tilde{\gamma}^{kl} \partial_l \chi) \Rightarrow \Gamma^k = \chi \tilde{\Gamma}^k + \frac{1}{2} \tilde{\gamma}^{kl} \partial_l \chi, \quad (2.42)$$

as an independent variable. In terms of the BSSN variables $\chi, \tilde{\gamma}_{ij}, \tilde{A}_{ij}, \tilde{\Gamma}^k$, the evolution equations are

$$(\partial_t - \mathcal{L}_\beta) \tilde{\gamma}_{ij} = -2\alpha \tilde{A}_{ij}, \quad (2.43a)$$

$$(\partial_t - \mathcal{L}_\beta) \chi = \frac{2}{3} \alpha \chi K, \quad (2.43b)$$

$$(\partial_t - \mathcal{L}_\beta) K = [\dots] + 4\pi \alpha (E + S), \quad (2.43c)$$

$$(\partial_t - \mathcal{L}_\beta) \tilde{A}_{ij} = [\dots] - 8\pi \alpha \left(\chi S_{ij} - \frac{S}{3} \tilde{\gamma}_{ij} \right), \quad (2.43d)$$

$$(\partial_t - \mathcal{L}_\beta) \tilde{\Gamma}^i = [\dots] - 16\pi \alpha \chi^{-1} j^i, \quad (2.43e)$$

where $[\dots]$ denotes the standard right-hand side of the BSSN equations in the absence of source terms (see *e.g.* [80]); the source terms are determined by

$$E \equiv n^\alpha n^\beta T_{\alpha\beta}, \quad (2.44)$$

$$j_i \equiv -\gamma_i^\alpha n^\beta T_{\alpha\beta}, \quad (2.45)$$

$$S_{ij} \equiv \gamma_i^\alpha \gamma_j^\beta T_{\alpha\beta}, \quad (2.46)$$

$$S \equiv \gamma^{ij} S_{ij}, \quad (2.47)$$

where the energy momentum tensor is given by Eq. (2.18). A straightforward computation shows that

$$\begin{aligned} \frac{4\pi(E+S)}{D-4} &= -(D-5)\lambda^{-1} + \frac{1}{2}\lambda^{-1}\chi^{3/2}\tilde{\gamma}^{ij}\tilde{D}_i\left(\chi^{-1/2}\partial_j\lambda\right) \\ &\quad + \frac{D-6}{4}\lambda^{-2}\chi\tilde{\gamma}^{ij}\partial_i\lambda\partial_j\lambda - \lambda^{-1}KK_\lambda - (D-5)\lambda^{-2}K_\lambda^2, \end{aligned} \quad (2.48a)$$

$$\begin{aligned} \frac{8\pi\chi\left(S_{ij}-\frac{S}{3}\gamma_{ij}\right)}{D-4} &= \frac{1}{2}\chi\lambda^{-1}\tilde{D}_i\partial_j\lambda + \frac{1}{4}\lambda^{-1}\left(\partial_i\lambda\partial_j\chi + \partial_j\lambda\partial_i\chi - \tilde{\gamma}^{kl}\tilde{\gamma}_{ij}\partial_k\lambda\partial_l\chi\right) - \frac{1}{4}\chi\lambda^{-2}\partial_i\lambda\partial_j\lambda \\ &\quad - \lambda^{-1}K_\lambda\tilde{A}_{ij} - \frac{1}{6}\tilde{\gamma}_{ij}\lambda^{-1}\chi^{3/2}\tilde{\gamma}^{kl}\tilde{D}_k\left(\chi^{-1/2}\partial_l\lambda\right) + \frac{1}{12}\tilde{\gamma}_{ij}\lambda^{-2}\chi\tilde{\gamma}^{kl}\partial_l\lambda\partial_k\lambda, \end{aligned} \quad (2.48b)$$

$$\frac{16\pi\chi^{-1}j^i}{D-4} = 2\lambda^{-1}\tilde{\gamma}^{ij}\partial_jK_\lambda - \lambda^{-2}K_\lambda\tilde{\gamma}^{ij}\partial_j\lambda - \tilde{\gamma}^{ik}\tilde{\gamma}^{lj}\tilde{A}_{kl}\lambda^{-1}\partial_j\lambda - \frac{\tilde{\gamma}^{ij}}{3}K\lambda^{-1}\partial_j\lambda, \quad (2.48c)$$

where \tilde{D}_i is the covariant derivative with respect to $\tilde{\gamma}_{ij}$.

Finally, the evolution equations for λ and K_λ are

$$(\partial_t - \mathcal{L}_\beta) \lambda = -2\alpha K_\lambda, \quad (2.49a)$$

$$\begin{aligned} (\partial_t - \mathcal{L}_\beta) K_\lambda = \alpha \left\{ (D-5) + \frac{6-D}{4} [\lambda^{-1} \chi \tilde{\gamma}^{ij} \partial_i \lambda \partial_j \lambda - 4\lambda^{-1} K_\lambda^2] \right. \\ \left. + K K_\lambda - \frac{1}{2} \chi^{3/2} \tilde{\gamma}^{kl} \tilde{D}_k (\chi^{-1/2} \partial_l \lambda) \right\} - \frac{1}{2} \chi \tilde{\gamma}^{ij} \partial_j \alpha \partial_i \lambda. \end{aligned} \quad (2.49b)$$

As stated before, in the case of head-on collisions of spinless BHs the full symmetry of the D dimensional system we want to consider makes equations (2.49) redundant, by virtue of (2.13). This allows to determine the quasi-matter degree of freedom in terms of the three dimensional spatial geometry, at each time slice. Indeed, we have only used an $SO(D-3)$ subgroup in the dimensional reduction we have performed. The extra symmetry manifests itself in the fact that γ_{ij} possesses, at all times, (at least) one Killing vector field. If one chooses coordinates adapted to this Killing vector field, $\partial/\partial\theta$, the metric can then be written in the form (2.12), and then the quasi-matter degree of freedom can be determined from the spatial geometry by (2.13). In the numerical implementation, one can either determine, at each time-step, the scalar field through (2.13), or impose (2.13) only in the initial data, and then evolve the scalar field using Eq. (2.49).

3. INITIAL DATA

Following the approach in [81, 82], we now derive the initial data of the evolution.

3.1. D dimensional Hamiltonian and momentum constraints

Let $\bar{\Sigma}$ be a $(D-1)$ -dimensional space-like hyper-surface with induced metric $\bar{\gamma}_{ab}$ and extrinsic curvature \bar{K}_{ab} in the D dimensional space-time. The space-time metric has the form

$$d\hat{s}^2 = \hat{g}_{MN} dx^M dx^N = -\alpha^2 dt^2 + \bar{\gamma}_{ab} (dx^a + \beta^a dt) (dx^b + \beta^b dt), \quad (3.1)$$

where lower case latin indices take values $a = 1, \dots, D-1$. The constraint equations are

$$\bar{R} + \bar{K}^2 - \bar{K}_{ab} \bar{K}^{ab} = 0, \quad (3.2)$$

$$\bar{D}_a (\bar{K}^{ab} - \bar{\gamma}^{ab} \bar{K}) = 0, \quad (3.3)$$

where \bar{R} is the Ricci scalar of the hyper-surface $\bar{\Sigma}$, \bar{K} is the trace of the extrinsic curvature and \bar{D}_a is the covariant derivative with respect to $\bar{\gamma}_{ab}$.

We conformally decompose the spatial metric

$$\bar{\gamma}_{ab} = \psi^{\frac{4}{D-3}} \hat{\gamma}_{ab}, \quad (3.4)$$

which introduces the conformal factor ψ , and split the extrinsic curvature in trace and trace-free parts,

$$\bar{K}_{ab} \equiv \bar{A}_{ab} + \frac{\bar{K}}{D-1} \bar{\gamma}_{ab}, \quad (3.5)$$

where $\bar{\gamma}^{ab} \bar{A}_{ab} = 0$. Define $\bar{A}^{ab} \equiv \bar{\gamma}^{ac} \bar{\gamma}^{bd} \bar{A}_{cd}$; define also the quantity

$$\hat{A}^{ab} \equiv \psi^{\frac{2(D+1)}{D-3}} \bar{A}^{ab}, \quad (3.6)$$

and lower its indices with $\hat{\gamma}_{ab}$,

$$\hat{A}_{ab} \equiv \hat{\gamma}_{ac} \hat{\gamma}_{bd} \hat{A}^{cd} = \psi^2 \bar{A}_{ab}. \quad (3.7)$$

Assuming that the ‘‘conformal metric’’ $\hat{\gamma}_{ab}$ is flat, which is a good approximation for the class of problems we want to study, we impose the ‘‘maximal slicing condition’’ $\bar{K} = 0$. Then, the Hamiltonian and momentum constraints become

$$\hat{\nabla}_a \hat{A}^{ab} = 0, \quad (3.8)$$

$$\hat{\Delta} \psi + \frac{D-3}{4(D-2)} \psi^{-\frac{3D-5}{D-3}} \hat{A}^{ab} \hat{A}_{ab} = 0, \quad (3.9)$$

where $\hat{\nabla}$ is the covariant derivative with respect to $\hat{\gamma}_{ab}$ and $\hat{\Delta}$ is the flat space Laplace operator.

3.2. Brill-Lindquist initial data and matching to four dimensions

The simplest way to solve the constraints (3.8)-(3.9) is to require the extrinsic curvature to be zero

$$\bar{K}_{ab} = 0. \quad (3.10)$$

This is sufficient to model the evolution of a single BH or even of N non-spinning, non-boosted BHs. The constraints reduce to a simple harmonic equation for the conformal factor, $\hat{\Delta} \psi = 0$, which we solve in cylindrical coordinates $\{x^a\} = (z, \rho, \theta, \dots)$, where ‘ \dots ’ represent the coordinates on the $(D-4)$ -sphere,

$$\hat{\gamma}_{ab} dx^a dx^b = dz^2 + d\rho^2 + \rho^2 (d\theta^2 + \sin^2 \theta d\Omega_{D-4}). \quad (3.11)$$

This choice of coordinates makes manifest the symmetries we want to impose. Observe that θ is a polar rather than an azimuthal coordinate, *i.e.* $\theta \in [0, \pi]$. Next, we introduce ‘‘incomplete’’ Cartesian coordinates as

$$x = \rho \cos \theta, \quad y = \rho \sin \theta, \quad (3.12)$$

where $-\infty < x < +\infty$ and $0 \leq y < +\infty$; we can then write the D dimensional initial data as (3.10) together with

$$\bar{\gamma}_{ab} dx^a dx^b = \psi^{\frac{4}{D-3}} [dx^2 + dy^2 + dz^2 + y^2 d\Omega_{D-4}], \quad (3.13)$$

where ψ is a harmonic function on (3.11).

If we compare the space-time metric (3.1) at the initial time slice, for which the spatial metric is given by (3.4) and (3.13), with the generic form that has an $SO(D-3)$ symmetry and is given by (2.14), (2.21), we see that the initial data for the four dimensional variables are

$$\gamma_{ij} dx^i dx^j = \psi^{\frac{4}{D-3}} [dx^2 + dy^2 + dz^2], \quad (3.14)$$

and

$$\lambda = y^2 \psi^{\frac{4}{D-3}}. \quad (3.15)$$

It remains to determine the initial conditions for K_{ij} and K_λ . Using a set of D dimensional coordinates that make manifest the $SO(D-3)$ isometry, such as the one used in (3.13), the vanishing of the extrinsic curvature \bar{K}_{ij} is equivalent to

$$K_{ij} = 0, \quad (3.16)$$

whereas the vanishing of the components of \bar{K}_{ab} along the $(D - 4)$ -sphere implies that

$$K_\lambda = 0. \quad (3.17)$$

Equations (3.14)–(3.17) represent the Brill-Lindquist initial data in our framework.

3.2.1. Evolution of a single black hole

As one test of our framework we study the case of a single, non-spinning BH. Even though the space-time is static, the slicing evolves when using the puncture gauge.

The solution for the conformal factor, which shall be used in the numerical tests to be presented below, is given by

$$\psi \equiv 1 + \frac{\mu^{D-3}}{4[x^2 + y^2 + (z - z_{BH})^2]^{(D-3)/2}}, \quad (3.18)$$

where the ‘‘puncture’’ [83] is placed at $x = y = 0$ and $z = z_{BH}$. In this formulation, there is an interesting signature that the BH we wish to evolve is higher dimensional: the fall off of ψ , which is that of a harmonic function in $D - 1$ spatial dimensions. Because the Tangherlini solution [69] may be expressed, in the same coordinate system as used in (3.13), as

$$d\hat{s}^2 = - \left(\frac{4R^{D-3} - \mu^{D-3}}{4R^{D-3} + \mu^{D-3}} \right)^2 dt^2 + \left(1 + \frac{\mu^{D-3}}{4R^{D-3}} \right)^{\frac{4}{D-3}} (dx^2 + dy^2 + dz^2 + y^2 d\Omega_{D-4}), \quad (3.19)$$

where $R = \sqrt{x^2 + y^2 + z^2}$, we conclude that the parameter μ appearing in the initial condition (3.18) is the same which appears in this form of the Tangherlini solution. It is related to the ADM mass by

$$\mu^{D-3} = \frac{16\pi M_{ADM}}{(D-2)A^{S^{D-2}}}. \quad (3.20)$$

Note, however, that this form of the Tangherlini solution is not appropriate for a comparison with the numerical data. Indeed, the evolution does not, in general, preserve the conformally flat slicing of the initial condition, which is the slicing used in this form of the Tangherlini solution. We shall return to this issue in Section 4.1.

3.2.2. Head-on collision of black holes

As another test of our formulation, and in particular of the numerical code’s long term stability, we also evolve a head-on collision of non-spinning non-boosted BHs. In this case, the initial data for the conformal factor are given by

$$\psi \equiv 1 + \frac{\mu_A^{D-3}}{4[x^2 + y^2 + (z - z_A)^2]^{(D-3)/2}} + \frac{\mu_B^{D-3}}{4[x^2 + y^2 + (z - z_B)^2]^{(D-3)/2}}. \quad (3.21)$$

This conformal factor is used in Section 4.1.

4. THE NUMERICAL TREATMENT

Our numerical simulations have been performed by adapting the `LEAN` code [68], initially designed for 3+1 vacuum space-times. The `LEAN` code is based on the `CACTUS` computational toolkit [84]. It employs the BSSN formulation of the Einstein equations [66, 67], uses the moving puncture method [2, 3], the `CARPET` package for mesh refinement [85, 86], the spectral solver described in [87] for 3+1 initial data and Thornburg’s `AHFINDERDIRECT` [88, 89]. Details about `LEAN` may be found in [68]. Here we focus on the numerical issues generated by the quasi-matter terms arising from the dimensional reduction by isometry.

We expect that the quasi-matter field λ has a y^2 fall off as $y \rightarrow 0$, that is, on the xz plane. This leads to divisions by zero on the right-hand side of the BSSN evolution equations, cf. (2.48). Since we expect all variables to remain regular on the xz plane, all divisions by y need to be cancelled by a corresponding fall off behaviour of the numerators. At $y = 0$, however, in order to implement this behaviour numerically, we need to isolate the irregular terms and evaluate expressions such as

$$\lim_{y \rightarrow 0} \frac{f}{y}, \quad (4.1)$$

where f is some example function which behaves like y^n with $n \geq 1$ near the xz plane. It is necessary, for this purpose, to formulate the equations in terms of variables which are manifestly regular at $y = 0$. We also prefer to apply a conformal re-scaling of λ and use the evolution variable

$$\zeta \equiv \frac{\chi}{y^2} \lambda. \quad (4.2)$$

As in (2.49), in order to obtain a first order evolution system in time, we introduce an auxiliary variable (see Appendix A):

$$K_\zeta \equiv -\frac{1}{2\alpha y^2} (\partial_t - \mathcal{L}_\beta)(\zeta y^2) = -\frac{1}{2\alpha} \left(\partial_t \zeta - \beta^m \partial_m \zeta + \frac{2}{3} \zeta \partial_m \beta^m - 2\zeta \frac{\beta^y}{y} \right). \quad (4.3)$$

The third term on the right-hand side arises from the fact that ζ is not a scalar, but a scalar density of weight $-2/3$. The inclusion of this term might not be necessary for a stable numerical implementation. For consistency with the rest of the BSSN variables, however, we decide to keep this form of K_ζ .

The quasi-matter terms (2.48), the quasi-matter evolution equations (2.49) and the constraints are recast in terms of ζ and K_ζ in Appendix A. In particular, we notice that

$$K_\lambda = \frac{y^2}{\chi} K_\zeta + \frac{1}{3} \frac{y^2 \zeta}{\chi} K. \quad (4.4)$$

A detailed analysis of the equations in terms of the variables ζ and K_ζ shows how all terms with an explicit dependence on $1/y^n$, $n \geq 1$ may be treated for numerical implementation. This is discussed in Appendix B.

4.1. Numerical results in $D = 5$

We first address the question of longevity of our simulations in $D = 5$. It is also of interest in this context to test the code’s capability to successfully merge a BH binary. For this purpose

we have evolved a head-on collision starting from rest. The initial conditions are those from Section 3.2.2 with

$$\mu_A^2 = \mu_B^2 \equiv \frac{\mu^2}{2}, \quad (4.5)$$

$$z_A = -z_B = 3.185 \mu, \quad (4.6)$$

and we use the grid setup (cf. Sec. II E of Ref. [68])

$$\{(512, 256, 128, 64, 32, 16, 8) \times (2, 1), h = 1/32\},$$

in units of μ . The gauge variables α and β^i are evolved according to the modified moving puncture conditions (A5) and (A6) with parameters $\eta_K = \eta_{K_\zeta} = 1.5$ and $\eta = 0.75$. We employ fourth order discretization in space and time and impose a floor value [2] for the variable $\chi = 10^{-4}$.

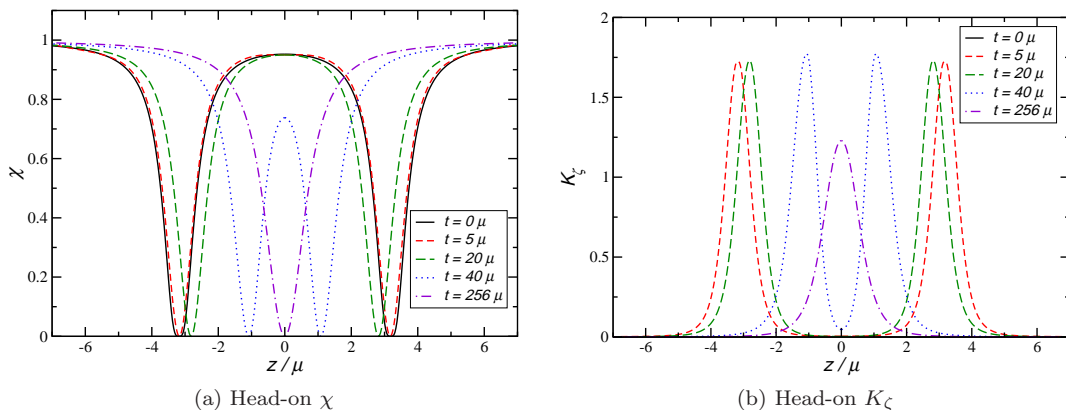


FIG. 2: The BSSN variable χ (left panel) and the quasi-matter momentum K_ζ (right panel) are shown along the axis of collision for a head-on collision at times $t = 0, 5, 20, 40$ and 256μ . Note that $K_\zeta = 0$ at $t = 0$.

In Fig. 2 we show the conformal factor χ and the momentum K_ζ along the axis of collision at various times. At early times, the evolution is dominated by the adjustment of the gauge (cf. the solid and short-dashed curves). The two holes next start approaching each other (long-dashed and dotted curves) and eventually merge and settle down into a single stationary hole (dash-dotted curves). We have not observed any signs of instability and decided to stop the simulation at $t = 256 \mu$. It is reassuring to notice that the framework can handle the merger in as robust a fashion as has been demonstrated by various numerical groups for BH binaries in 3+1 dimensions.

We have also used the head-on collision to test the relation between the scalar field λ and the $3 + 1$ metric discussed in Sec. 1.3 for the case that $SO(D - 2)$ is the full isometry group. We have verified for this purpose that Eq. 2.13 remains satisfied to within a relative error of 10^{-3} in the immediate vicinity of the puncture and at most 10^{-5} everywhere else.

In order to further test our numerical framework, we have performed simulations of a single BH, using the initial data described in Section 3.2.1 and the grid setup

$$\{(512, 256, 128, 64, 32, 16, 8, 4, 2) \times (), h\},$$

in units of μ with resolutions $h_c = 1/32$ and $h_f = 1/48$. In Fig. 3 we show the Hamiltonian constraint and the y component of the momentum constraint at evolution time $t = 28\mu$. By this time there is hardly any more gauge dynamics going on. One can see that there is some

noise, but the overall convergence is acceptable. For the Hamiltonian constraint the convergence is essentially 4th order and for the momentum constraint it decreases slightly towards 2nd or 3rd order in patches. From experience in 3+1 dimensional numerical relativity this is perfectly acceptable, especially given the fact that prolongation in time is second-order accurate.

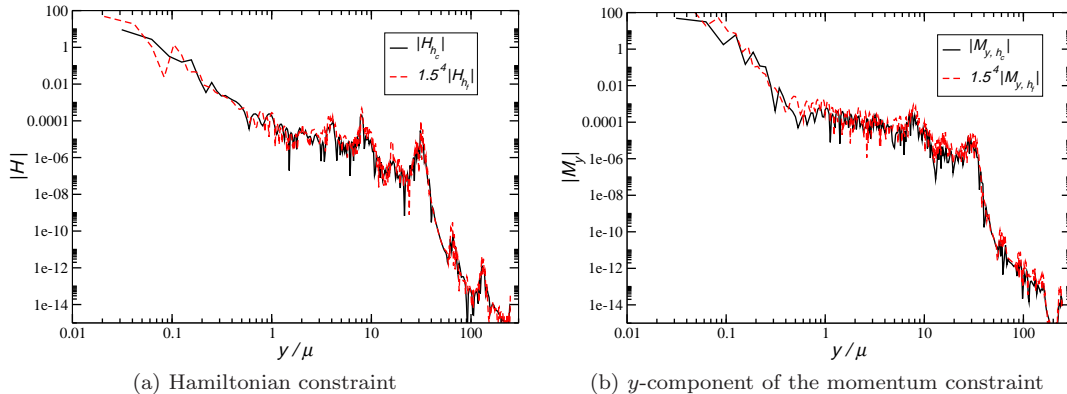


FIG. 3: Constraints at time $t = 28\mu$, for the evolution of a single Tangherlini BH in five dimensions.

A different test of our numerical code was performed in order to compare the analytical Tangherlini solution with our numerical results. The challenge to do this comparison, at the level of the line element, is to write the well known analytical solution in the same coordinate system in which the numerical evolution is occurring. One way around this problem is to fix the numerical gauge as to match a known coordinate system for the analytic solution. Following [64] we fixed the gauge parameters to be

$$\alpha = 1, \quad \beta^i = 0, \quad i = 1, 2, 3; \quad (4.7)$$

this corresponds to *geodesic slicing*. The D dimensional Tangherlini solution may be expressed in a coordinate system of type (3.1) with $\alpha = 1, \beta^a = 0, a = 1, \dots, D-1$. This coordinate system may be achieved by setting a congruence of in-falling radial time-like geodesics, each geodesic starting from rest at radial coordinate r_0 , with r_0 spanning the interval $[\mu, +\infty[$, and using their proper time τ and r_0 as coordinates (instead of the standard t, r Schwarzschild-like coordinates). A detailed construction of the Tangherlini solution in these coordinates is given in Appendix C. The line element becomes

$$ds^2 = -d\tau^2 + \frac{\left(r_0(R)^2 + \left(\frac{\mu}{r_0(R)}\right)^2 \tau^2\right)^2}{r_0(R)^2 - \left(\frac{\mu}{r_0(R)}\right)^2 \tau^2} \frac{dR^2}{R^2} + \left(r_0(R)^2 - \left(\frac{\mu}{r_0(R)}\right)^2 \tau^2\right) d\Omega_3, \quad (4.8)$$

where $r_0(R)$ is given by Eq. (C5).

The numerical evolution in this gauge is naturally doomed. Geodesics hit the physical singularity at finite proper time. Thus, this slicing is inappropriate for a long term numerical evolution. As long as the evolution does not break down, however, there is perfect control over the slicing, and hence the numerical and analytical evolution can be compared with ease. This is shown in Fig. 4, where we have plotted one metric component $\tilde{\gamma}_{xx}$ along the x axis (left) and ζ/χ (right), for various values of τ using both the analytical solution and numerical data. The agreement is excellent for $\tilde{\gamma}_{xx}$ and good for ζ/χ . The latter shows some deviations very close to the puncture, but we believe that it is not a problem for two reasons: (i) the agreement improves for higher resolution; (ii) the mismatch does not propagate outside of the horizon.

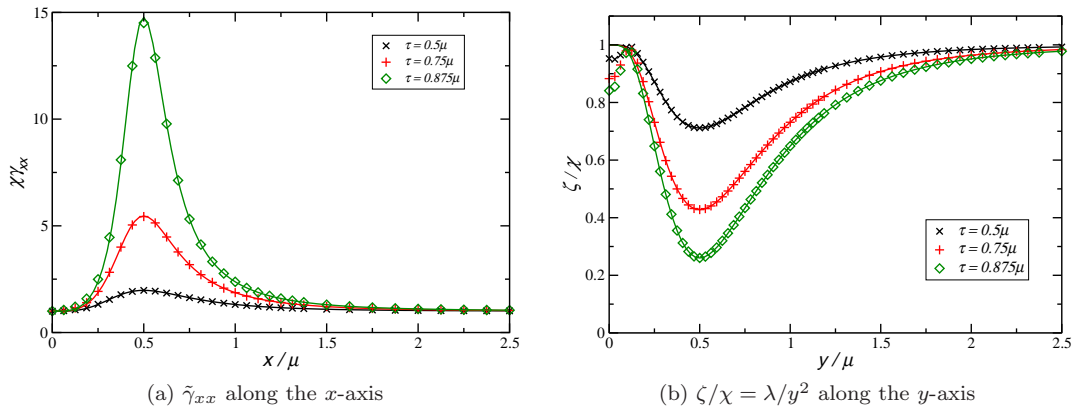


FIG. 4: Numerical values versus analytical plot (solid lines) for various values of τ , for the single Tangherlini BH in five dimensions. The horizontal axes are labelled in units of μ .

It is easy to interpret the behaviour observed for $\tilde{\gamma}_{xx}$. The geodesic that starts from $r = r_0$ (in Schwarzschild-like coordinates) hits the physical singularity of the Tangherlini solution within proper time $\tau = r_0^2/\mu$. Moreover, this happens at

$$R = \frac{\mu}{2} \frac{1}{\sqrt{\tau/\mu} \pm \sqrt{\tau/\mu - 1}}. \quad (4.9)$$

The earliest time at which the slicing hits the singularity is $\tau = \mu$, which happens at $R = \mu/2$. On the x -axis $R = x$ and indeed one sees in Fig. 4 that $\tilde{\gamma}_{xx}$ diverges at $x = \mu/2$. The divergence then extends to both larger and smaller values of x , as expected from (4.9).

4.2. Preliminary numerical results in $D = 6$

A quick glance at the evolution equations (A7a) and (A7b) of the scalar field ζ as well as the source terms (A8a)-(A8c) indicates that $D = 5$ may be a special case. In all these expressions there exist terms which manifestly vanish for $D = 5$. In contrast, there exist no terms which manifestly vanish for any dimension $D \geq 6$. The purpose of this Section is to extend the test of our framework to a case which involves all source terms.

We have indeed noticed one fundamental difference between simulations in $D = 5$ and those using $D \geq 6$. Whereas we have been able to obtain stable simulations of single BHs lasting hundreds of μ for the former case by modifying the moving puncture gauge conditions, we have not yet succeeded in doing so for $D \geq 6$. While the lifetime of the simulations in $D \geq 6$ shows a dependence on the exact nature of lapse and shift, all simulations developed instabilities on a timescale of about 10μ . Resolving this issue requires an extensive study involving a large number of experiments with gauge conditions, constraint damping and possibly other aspects of the formulation. Such a study is beyond the scope of this work and deferred to a future publication. The results presented in this Section still provide valuable information. Most importantly, they demonstrate the internal consistency of the code for $D \geq 6$ and thus minimise the possibility of a simple error in the implementation. Furthermore they exhibit clearly that our framework and in particular our regularisation of the variables as discussed in Appendix B is in principle suitable for simulations in arbitrary dimensions.

We first consider the convergence of the constraints analogous to the results displayed in Fig. 3 for $D = 5$. Compared to those simulations, the only change we have applied in $D = 6$ is to set

the gauge parameters to $\eta_K = \eta_{K_\zeta} = \eta = 2$. This choice enables us to evolve single BHs to about 10μ when instabilities cause the runs to abort. In Fig. 5 we show the Hamiltonian and

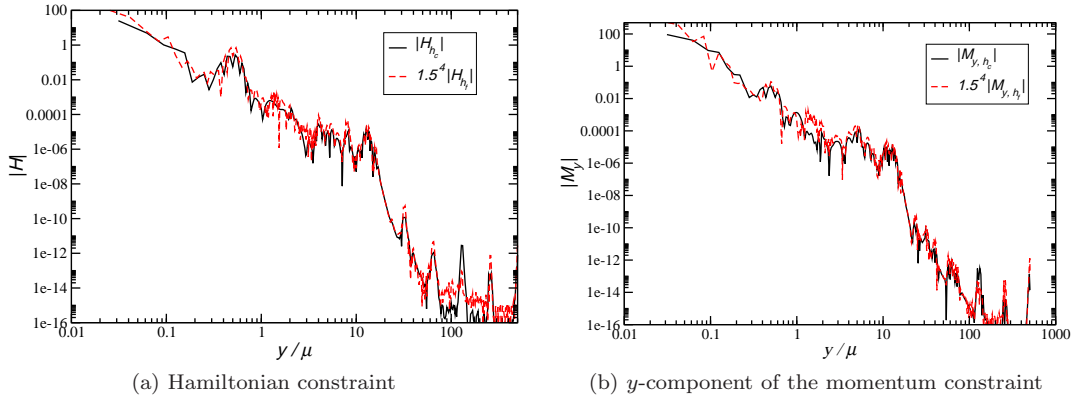


FIG. 5: Constraints at time $t = 8\mu$, for the evolution of a single Tangherlini BH in six dimensions.

the y -component of the momentum constraint at $t = 8 \mu$ along the y -axis. As for $D = 5$, the high resolution result is amplified by a factor 1.5^4 expected for fourth order convergence [80]. While the convergence appears to be closer to second order in some patches of the momentum constraint, the results are clearly compatible with the numerical discretization.

For the second test, we compare the numerical evolution of a single $D = 6$ Tangherlini BH with the analytic solution, using geodesic slicing. This comparison is more difficult in the present case than in $D = 5$, because the line element analogous to (4.8) cannot be obtained in a simple

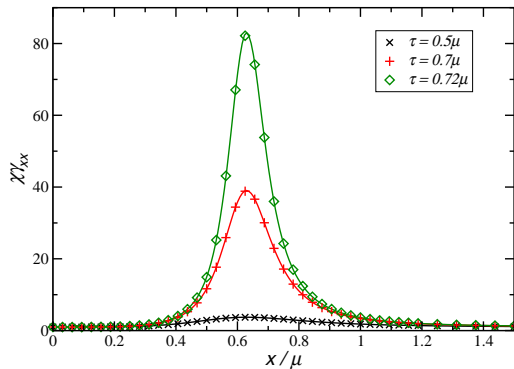


FIG. 6: Numerical values versus the semi-analytic expression of $\tilde{\gamma}_{xx}$ (cf. Appendix C) along the x -axis for the single Tangherlini BH in six dimensions.

analytic form. In Appendix C we demonstrate how a semi-analytic solution can be obtained for the metric. In Fig. 6 we compare this expression with the three dimensional numerical values at times $\tau = 0.5 \mu$, 0.7μ and 0.72μ . The agreement is excellent and demonstrates that our code works well at least up to the point where instabilities set in. As mentioned above, resolving these stability problems will be of the highest priority in future extensions of our work.

5. FINAL REMARKS

In this paper we present a framework that allows the generalisation of the present generation of 3+1 numerical codes to evolve, with relatively minor modifications, space-times with $SO(D-2)$ symmetry in 5 dimensions and $SO(D-3)$ symmetry in $D \geq 6$ dimensions. The key idea is a dimensional reduction of the problem along the lines of Geroch's [70] procedure that recasts the D dimensional Einstein vacuum equations in the form of the standard four dimensional equations plus some quasi-matter source terms. The resulting equations can be transformed straightforwardly into the BSSN formulation that has proved remarkably successful in numerical evolutions of BH configurations in 3+1 space-times. We have isolated several issues related to the regularisation of the variables used in our formulation and demonstrated how all difficulties related to the coordinate singularity arising out of the use of a "radius-like" coordinate can be successfully addressed in a numerical implementation. We have further illustrated how initial data for single, non-spinning BHs as well as BH binaries with vanishing initial extrinsic curvature can be adapted straightforwardly to the formulation presented in this paper. More generally, the class of problems that may be studied with our framework includes head-on collisions in $D \geq 5$ and a subset of BH collisions with impact parameter and spin in $D \geq 6$.

As might be expected, stable evolutions of such space-times require some modifications of the underlying methods of the so-called *moving puncture* technique, especially with regard to the gauge conditions used therein. We have successfully modified the slicing condition via incorporation of the canonical momentum of the quasi-matter field in order to obtain long-term stable simulations in $D = 5$ dimensions. Unfortunately, these modifications do not appear sufficient to provide long-term stability for arbitrary values of the dimensionality D . We will address this important issue in the form of a systematic study in future work.

We have tested our framework by adapting the LEAN code and performed a variety of single BH space-times. Most importantly, we have demonstrated the internal consistency of our numerical framework in $D = 5$ and 6 dimensions by showing convergence of the Hamiltonian and momentum constraints as well as comparing numerical results with (semi-)analytic expressions for a single Tangherlini BH in geodesic slicing. We have further shown for $D = 5$ that the head-on collision of a BH binary successfully merges into a single hole which settles down into a stationary state and can be evolved numerically for long times, hundreds of μ in the present example.

A complete study of such BH binary evolutions requires the implementation of gravitational wave extraction in arbitrary dimensions as well as the generalisation of apparent horizon diagnostics beyond $D = 4$. Both are currently being implemented in the LEAN code and will be discussed in detail in future work.

In spite of several open questions, we believe that our formalism will open up a vast range of uncharted territory in BH physics for contemporary numerical relativity. The list of possible applications and extensions of our framework is too large to be included here, and we merely mention strong hyperbolicity studies of the BSSN formulation with sources and systematic investigation of BH binary dynamics in D dimensions. These studies are under way and will be reported elsewhere.

Acknowledgments

We would like to thank L. Lindblom and M. Sampaio for discussions. We also thank the participants of the V Iberian Cosmology Meeting, the XII Marcel Grossmann Meetings, the Spanish Relativity Meeting and the I and II Black Holes Workshop for useful feedback. M.Z. and H.W. are funded by FCT through grants SFRH/BD/43558/2008 and SFRH/BD/46061/2008. V.C. acknowledges financial support from Fundação Calouste Gulbenkian through a short-term scholarship. V.C. and C.H. are supported by a "Ciência 2007" research contract. A.N. is funded by FCT

through grant SFRH/BPD/47955/2008. This work was partially supported by FCT - Portugal through projects PTDC/FIS/64175/2006, PTDC/FIS/098025/2008, PTDC/FIS/098032/2008 PTDC/CTE-AST/098034/2008, CERN/FP/109306/2009, CERN/FP/109290/2009 as well as NSF grants PHY-090003, PHY-0900735, PHY-0601459, PHY-0652995 and the Fairchild foundation to Caltech. Computations were performed on the TeraGrid clusters ranger and kraken and at Magerit in Madrid. The authors thankfully acknowledge the computer resources, technical expertise and assistance provided by the Barcelona Supercomputing Centre — Centro Nacional de Supercomputación.

Appendix A: Implementing regular variables

The numerical evolution faces a problem at the symmetry axis, given the quasi-matter terms in (2.48) and the initial data discussed in Sec. 3. The “incomplete” Cartesian coordinate y vanishes at the symmetry axis, cf. (3.12). Then, from (3.15), λ vanishes at the axis (except, possibly, at the puncture). Inspection of equations (2.48) and (2.49) immediately reveals various divisions by λ , leading to numerical problems.

From previous experience with polar and spherical coordinates in simpler models involving, for example, neutron stars (cf. [90, 91]) we know that it is better to avoid the use of singular variables such as λ . We should use, instead, regular functions. In our case, since λ behaves as y^2 near the axis, this is simply achieved by introducing a variable ζ via (4.2). The evolution of ζ is formulated in terms of a first order in time system of equations. For this purpose we have introduced in Eq. (4.3) the variable K_ζ . We remark that if, instead, we employ the standard definition for the momentum associated with ζ , *i.e.*

$$\hat{K}_\zeta \equiv -\frac{1}{2\alpha}(\partial_t - \mathcal{L}_\beta)\zeta = -\frac{1}{2\alpha} \left(\partial_t \zeta - \beta^m \partial_m \zeta + \frac{2}{3} \zeta \partial_m \beta^m \right), \quad (\text{A1})$$

we face problems in the numerical evolution for vanishing lapse. This may be seen as follows. From (4.4)

$$K_\lambda = \frac{y^2}{\chi} \hat{K}_\zeta + \frac{1}{3} \frac{y^2 \zeta}{\chi} K + \frac{\beta^y y \zeta}{\alpha \chi}. \quad (\text{A2})$$

Acting on both sides of this equation with the derivative operator

$$\partial_0 \equiv \partial_t - \beta^m \partial_m,$$

results in the expression

$$\begin{aligned} \partial_0 \hat{K}_\zeta &= \frac{\chi}{y^2} \partial_0 K_\lambda + 4 \frac{\beta^y}{y} \hat{K}_\zeta + \frac{4}{3} \alpha K \hat{K}_\zeta + \frac{4}{3} \zeta \frac{\beta^y}{y} K + \frac{2}{9} \zeta \alpha K^2 \\ &\quad - \frac{\zeta}{3} \partial_0 K + \frac{\zeta}{\alpha} \left(\frac{\beta^y}{y} \right)^2 - \frac{2}{3} \hat{K}_\zeta \partial_m \beta^m - \frac{\zeta}{\alpha} \frac{\partial_0 \beta^y}{y} + \zeta \frac{\beta^y}{y \alpha^2} \partial_0 \alpha. \end{aligned} \quad (\text{A3})$$

This is an evolution equation for \hat{K}_ζ . To obtain it explicitly one uses (2.37) to express $\partial_0 K_\lambda$, together with

$$\partial_0 K = -D^m \partial_m \alpha + \alpha \left(\tilde{A}^{mn} \tilde{A}_{mn} + \frac{1}{3} K^2 \right) + 4\pi \alpha (E + S). \quad (\text{A4})$$

Moreover we need gauge conditions. Throughout this work we use the following coordinate choices

$$\partial_0 \alpha = -2\alpha(\eta_K K + \eta_{K_\zeta} K_\zeta), \quad (\text{A5})$$

$$\partial_0 \beta^i = \frac{3}{4} \tilde{\Gamma}^i - \eta \beta^i. \quad (\text{A6})$$

Note the extra term involving K_ζ in the slicing condition compared with standard moving puncture gauge in 3+1 dimensions and the additional freedom we have introduced in the form of the parameters η_K and η_{K_ζ} .

The problems in the case of a collapsed lapse become clear if we consider the final two terms in (A3). These terms do not change when BSSN variables are introduced and diverge for the modified moving puncture gauge conditions (A5) and (A6) as the lapse $\alpha \rightarrow 0$. We have solved this problem by expressing our equations in terms of the variable K_ζ (4.3), instead of \hat{K}_ζ .

In BSSN variables, the evolution equation for ζ and K_ζ (which replace the quasi-matter evolution equations (2.49)) become

$$\partial_t \zeta = -2\alpha K_\zeta + \beta^m \partial_m \zeta - \frac{2}{3} \zeta \partial_m \beta^m + 2\zeta \frac{\beta^y}{y}, \quad (\text{A7a})$$

$$\begin{aligned} \partial_t K_\zeta = & \beta^m \partial_m K_\zeta - \frac{2}{3} K_\zeta \partial_m \beta^m + 2 \frac{\beta^y}{y} K_\zeta - \frac{1}{3} \zeta \partial_0 K - \frac{\chi \zeta}{y} \tilde{\gamma}^{ym} \partial_m \alpha - \frac{1}{2} \tilde{\gamma}^{mn} (\partial_m \alpha) (\chi \partial_n \zeta - \zeta \partial_n \chi) \\ & + \alpha \left[(5-D) \frac{\chi}{y^2} (\zeta \tilde{\gamma}^{yy} - 1) + (4-D) \frac{\chi}{y} \tilde{\gamma}^{ym} \partial_m \zeta + \frac{2D-7}{2} \frac{\zeta}{y} \tilde{\gamma}^{ym} \partial_m \chi \right. \\ & + \frac{6-D}{4} \frac{\chi}{\zeta} \tilde{\gamma}^{mn} (\partial_m \zeta) (\partial_n \zeta) + \frac{2D-7}{4} \tilde{\gamma}^{mn} (\partial_m \zeta) (\partial_n \chi) + \frac{1-D}{4} \frac{\zeta}{\chi} \tilde{\gamma}^{mn} (\partial_m \chi) (\partial_n \chi) \\ & \left. + (D-6) \frac{K_\zeta^2}{\zeta} + \frac{2D-5}{3} K K_\zeta + \frac{D-1}{9} \zeta K^2 + \frac{1}{2} \tilde{\gamma}^{mn} (\zeta \tilde{D}_m \partial_n \chi - \chi \tilde{D}_m \partial_n \zeta) + \chi \zeta \frac{\tilde{\Gamma}^y}{y} \right]. \end{aligned} \quad (\text{A7b})$$

These equations have no manifest problems as $\alpha \rightarrow 0$.

In terms of the regular variables, ζ and K_ζ , the quasi-matter terms (2.48) read

$$\begin{aligned} \frac{4\pi(E+S)}{D-4} &= (D-5)\frac{\chi}{\zeta}\frac{\tilde{\gamma}^{yy}\zeta-1}{y^2} - \frac{2D-7}{4\tilde{\kappa}}\tilde{\gamma}^{mn}(\partial_m\zeta)(\partial_n\chi) - \chi\frac{\tilde{\Gamma}^y}{y} \\ &\quad + \frac{D-6}{4}\frac{\chi}{\zeta^2}\tilde{\gamma}^{mn}(\partial_m\zeta)(\partial_n\zeta) + \frac{1}{2\zeta}\tilde{\gamma}^{mn}(\chi\tilde{D}_m\partial_n\zeta - \zeta\tilde{D}_m\partial_n\chi) \\ &\quad - \frac{KK_\zeta}{\zeta} - \frac{1}{3}K^2 + (D-4)\frac{\tilde{\gamma}^{ym}}{y}\left(\frac{\chi}{\zeta}\partial_m\zeta - \partial_m\chi\right) - \frac{1}{2}\frac{\tilde{\gamma}^{ym}}{y}\partial_m\chi \\ &\quad + \frac{D-1}{4}\tilde{\gamma}^{mn}\frac{(\partial_m\chi)(\partial_n\chi)}{\chi} - (D-5)\left(\frac{K_\zeta}{\zeta} + \frac{K}{3}\right)^2, \end{aligned} \quad (\text{A8a})$$

$$\begin{aligned} \frac{8\pi\chi(S_{ij} - \frac{1}{3}\gamma_{ij}S)}{D-4} &= \frac{1}{2}\left[\frac{\chi}{y\zeta}\left(\delta_j^y\partial_i\zeta + \delta_i^y\partial_j\zeta - 2\zeta\tilde{\Gamma}_{ij}^y\right) + \frac{1}{2\chi}(\partial_i\chi)(\partial_j\chi) + \frac{\chi}{\zeta}\tilde{D}_i\partial_j\zeta\right. \\ &\quad \left. - \tilde{D}_i\partial_j\chi + \frac{1}{2\chi}\tilde{\gamma}_{ij}\tilde{\gamma}^{mn}\partial_n\chi\left(\partial_m\chi - \frac{\chi}{\zeta}\partial_m\zeta\right) - \tilde{\gamma}_{ij}\frac{\tilde{\gamma}^{ym}}{y}\partial_m\chi\right. \\ &\quad \left. - \frac{\chi}{2\zeta^2}(\partial_i\zeta)(\partial_j\zeta)\right]^{\text{TF}} - \left(\frac{K_\zeta}{\zeta} + \frac{1}{3}K\right)\tilde{A}_{ij}, \end{aligned} \quad (\text{A8b})$$

$$\begin{aligned} \frac{16\pi j_i}{D-4} &= \frac{2}{y}\left[\delta_i^y\frac{K_\zeta}{\zeta} - \tilde{\gamma}^{ym}\tilde{A}_{mi}\right] + 2\frac{1}{\zeta}\partial_i K_\zeta - \frac{K_\zeta}{\zeta}\left(\frac{1}{\chi}\partial_i\chi + \frac{1}{\zeta}\partial_i\zeta\right) \\ &\quad + \frac{2}{3}\partial_i K - \tilde{\gamma}^{nm}\tilde{A}_{mi}\left(\frac{1}{\zeta}\partial_n\zeta - \frac{1}{\chi}\partial_n\chi\right). \end{aligned} \quad (\text{A8c})$$

Finally, the constraints are now given by

$$\mathcal{H} \equiv R + \frac{2}{3}K^2 - \tilde{\gamma}^{mn}\tilde{\gamma}^{kl}\tilde{A}_{mk}\tilde{A}_{nl} - 16\pi E, \quad (\text{A9})$$

$$\mathcal{M}_i \equiv \tilde{\gamma}^{mn}\left(\tilde{D}_n\tilde{A}_{im} - \frac{3}{2}\tilde{A}_{mi}\frac{\partial_n\chi}{\chi}\right) - \frac{2}{3}\partial_i K - 8\pi j_i, \quad (\text{A10})$$

where we also need to express E in terms of our fundamental variables. It is given by

$$\begin{aligned} \frac{16\pi E}{D-4} &= (D-3)\frac{\chi}{y\zeta}\tilde{\gamma}^{ym}\partial_m\zeta - (D-2)\frac{1}{y}\tilde{\gamma}^{ym}\partial_m\chi + \frac{D-7}{4}\frac{\chi}{\zeta^2}\tilde{\gamma}^{mn}(\partial_m\zeta)(\partial_n\zeta) \\ &\quad - \frac{D-2}{2\zeta}\tilde{\gamma}^{mn}(\partial_m\zeta)(\partial_n\chi) + \frac{D+3}{4\chi}\tilde{\gamma}^{mn}(\partial_m\chi)(\partial_n\chi) - (D-5)\frac{K_\zeta^2}{\zeta^2} - \frac{2D-4}{3}K\frac{K_\zeta}{\zeta} \\ &\quad - \frac{D+1}{9}K^2 + \frac{\chi}{\zeta}\tilde{\gamma}^{mn}\tilde{D}_m\partial_n\zeta - \tilde{\gamma}^{mn}\tilde{D}_m\partial_n\chi - 2\chi\frac{\tilde{\Gamma}^y}{y} + (D-5)\frac{\chi}{\zeta}\frac{\tilde{\gamma}^{yy}\zeta-1}{y^2}. \end{aligned} \quad (\text{A11})$$

Appendix B: Analysis of troublesome terms at $y=0$

The right-hand sides of Eqs. (A7)-(A10) contain various terms which cannot be evaluated directly at $y=0$ because they involve explicit division by y . Although these terms are regular by virtue of a corresponding behaviour of the numerators, they need to be explicitly evaluated in the numerical implementation. In this Appendix we outline how the regularity of these terms can be implemented in a simple and efficient manner. For convenience we use a special notation: late latin indices i, j, \dots run from 1 to 3, covering x, y and z , but early latin indices a, b, \dots take values 1 and 3 but not 2, *i.e.* they cover x and z but not y .

We begin this discussion by describing a simple manipulation which underlies most of our regularisation procedure. Consider for this purpose a function h which is linear in y near $y = 0$, *i.e.* its Taylor expansion is given by $h(y) = h_1 y + \mathcal{O}(y^2)$. From this relation we directly obtain

$$\lim_{y \rightarrow 0} \frac{h}{y} = h_1 = \partial_y h. \quad (\text{B1})$$

This trading of divisions by y for partial derivatives extends to higher orders in a straightforward manner and will be used throughout the following discussion.

Next, we consider the right-hand sides of Eqs. (A7)-(A10) and summarise the potentially troublesome terms as follows

$$\frac{\beta^y}{y}, \quad \frac{\tilde{\Gamma}^y}{y}, \quad (\text{B2})$$

$$\frac{\tilde{\gamma}^{ym}}{y} \partial_m f, \quad (\text{B3})$$

$$\frac{\tilde{\gamma}^{yy} \zeta - 1}{y^2}, \quad (\text{B4})$$

$$\frac{1}{y} \left(\delta_i^y \frac{K_\zeta}{\zeta} - \tilde{\gamma}^{ym} \tilde{A}_{mi} \right), \quad (\text{B5})$$

$$\frac{1}{y} \left(\delta_j^y \partial_i \zeta + \delta_i^y \partial_j \zeta - 2\zeta \tilde{\Gamma}_{ij}^y \right). \quad (\text{B6})$$

Here f stands for either of the scalars or densities ζ , χ and α .

Regularity of the terms (B2) immediately follows from the symmetry condition of the y -component of a vector

$$\beta^y(-y) = -\beta^y(y). \quad (\text{B7})$$

We can therefore use the idea illustrated in Eq. (B1) and obtain

$$\lim_{y \rightarrow 0} \frac{\beta^y}{y} = \partial_y \beta^y, \quad (\text{B8})$$

and likewise for $\tilde{\Gamma}^y/y$. The terms (B3) are treated in a similar manner because the derivative of a scalar (density) behaves like a vector on our Cartesian grid. We thus obtain

$$\lim_{y \rightarrow 0} \left(\frac{\tilde{\gamma}^{ym}}{y} \partial_m f \right) = (\partial_y \tilde{\gamma}^{ya}) (\partial_a f) + \tilde{\gamma}^{yy} \partial_y \partial_y f. \quad (\text{B9})$$

Regularity of the expression (B4) is not immediately obvious but can be shown to follow directly from the requirement that there should be no conical singularity at $y = 0$. Specifically, this condition implies that $\tilde{\gamma}^{yy} \zeta = 1 + \mathcal{O}(y^2)$, so that

$$\lim_{y \rightarrow 0} \left(\frac{\tilde{\gamma}^{yy} \zeta - 1}{y^2} \right) = \frac{1}{2} (\zeta \partial_y \partial_y \tilde{\gamma}^{yy} + \tilde{\gamma}^{yy} \partial_y \partial_y \zeta). \quad (\text{B10})$$

The discussion of the term (B5) requires us to distinguish between the cases $i = a \neq y$ and $i = y$. The former straightforwardly results in

$$\lim_{y \rightarrow 0} \left(-\frac{\tilde{\gamma}^{ym}}{y} \tilde{A}_{ma} \right) = -\tilde{A}_{ba} \partial_y \tilde{\gamma}^{yb} - \tilde{\gamma}^{yy} \partial_y \tilde{A}_{ya}. \quad (\text{B11})$$

For the case $i = y$, we first note that the limit $y \rightarrow 0$ implies $\tilde{\gamma}^{yy} = 1/\tilde{\gamma}_{yy} + \mathcal{O}(y^2)$, so that the condition (B10), *i.e.* no conical singularities, can be written as

$$\lim_{y \rightarrow 0} (\zeta - \tilde{\gamma}_{yy}) = \mathcal{O}(y^2). \quad (\text{B12})$$

Next we take the time derivative of this expression and obtain after some manipulation

$$\mathcal{O}(y^2) = \lim_{y \rightarrow 0} \partial_t (\zeta - \tilde{\gamma}_{yy}) = -2\alpha\zeta \left(\frac{K_\zeta}{\zeta} - \tilde{\gamma}^{ym} \tilde{A}_{my} \right) + \mathcal{O}(y^2), \quad (\text{B13})$$

and, consequently,

$$\lim_{y \rightarrow 0} \left[\frac{1}{y} \left(\frac{K_\zeta}{\zeta} - \tilde{\gamma}^{ym} \tilde{A}_{my} \right) \right] = 0. \quad (\text{B14})$$

Finally, we consider the term (B6). Expansion of the Christoffel symbol, repeated use of the method illustrated in Eq. (B1) and the condition for avoiding a conical singularity enable us to regularise this term for all combinations of the free indices i and j . We thus obtain

$$\lim_{y \rightarrow 0} \left[\frac{1}{y} \left(2\partial_y \zeta - 2\zeta \tilde{\Gamma}_{yy}^y \right) \right] = 2\partial_y \partial_y \zeta - \zeta \tilde{\gamma}^{yy} \partial_y \partial_y \tilde{\gamma}_{yy} - \zeta (\partial_y \tilde{\gamma}^{yc}) (2\partial_y \tilde{\gamma}_{yc} - \partial_c \tilde{\gamma}_{yy}), \quad (\text{B15})$$

$$\lim_{y \rightarrow 0} \left[\frac{1}{y} \left(\partial_a \zeta - 2\zeta \tilde{\Gamma}_{ay}^y \right) \right] = 0, \quad (\text{B16})$$

$$\begin{aligned} \lim_{y \rightarrow 0} \left[-2 \frac{\zeta}{y} \tilde{\Gamma}_{ab}^y \right] &= -\zeta \tilde{\gamma}^{yy} (\partial_y \partial_a \tilde{\gamma}_{by} + \partial_y \partial_b \tilde{\gamma}_{ya} - \partial_y \partial_y \tilde{\gamma}_{ab}) \\ &\quad - \zeta (\partial_y \tilde{\gamma}^{yc}) (\partial_a \tilde{\gamma}_{bc} + \partial_b \tilde{\gamma}_{ac} - \partial_c \tilde{\gamma}_{ab}). \end{aligned} \quad (\text{B17})$$

We conclude this discussion with a method to express derivatives of the inverse metric in terms of derivatives of the metric. For this purpose we use the condition that $\det \tilde{\gamma}_{ij} = 1$ by construction and explicitly invert the metric components as for example in

$$\tilde{\gamma}^{xy} = \tilde{\gamma}_{xz} \tilde{\gamma}_{yz} - \tilde{\gamma}_{xy} \tilde{\gamma}_{zz}. \quad (\text{B18})$$

A straightforward calculation gives us the derivatives of the inverse metric components as follows

$$\partial_y \tilde{\gamma}^{xy} = \tilde{\gamma}_{xz} \partial_y \tilde{\gamma}_{yz} - \tilde{\gamma}_{zz} \partial_y \tilde{\gamma}_{xy} + \mathcal{O}(y^2), \quad (\text{B19})$$

$$\partial_y \tilde{\gamma}^{yz} = \tilde{\gamma}_{xz} \partial_y \tilde{\gamma}_{xy} - \tilde{\gamma}_{xx} \partial_y \tilde{\gamma}_{yz} + \mathcal{O}(y^2), \quad (\text{B20})$$

$$\partial_y \tilde{\gamma}^{yy} = \tilde{\gamma}_{zz} \partial_y \tilde{\gamma}_{xx} + \tilde{\gamma}_{xx} \partial_y \tilde{\gamma}_{zz} - 2\tilde{\gamma}_{xz} \partial_y \tilde{\gamma}_{xz}, \quad (\text{B21})$$

$$\partial_y \partial_y \tilde{\gamma}^{yy} = \tilde{\gamma}_{zz} \partial_y \partial_y \tilde{\gamma}_{xx} + \tilde{\gamma}_{xx} \partial_y \partial_y \tilde{\gamma}_{zz} - 2\tilde{\gamma}_{xz} \partial_y \partial_y \tilde{\gamma}_{xz} + \mathcal{O}(y^2). \quad (\text{B22})$$

The benefit in using these expressions is purely numerical: we do not need to store the inverse metric in grid functions which reduces the memory requirements of the simulations.

Appendix C: Geodesic slicing

In standard Schwarzschild-like coordinates, the Tangherlini metric reads

$$ds^2 = -f(r)dt^2 + \frac{dr^2}{f(r)} + r^2 d\Omega_{D-2}, \quad f(r) = 1 - \left(\frac{\mu}{r} \right)^{D-3}. \quad (\text{C1})$$

For a radially in-falling massive particle, starting from rest at $r = r_0$, the energy per unit mass is $\sqrt{f(r_0)}$. The geodesic equation may then be written as

$$\frac{dt}{d\tau} = \frac{\sqrt{f(r_0)}}{f(r)}, \quad \left(\frac{dr}{d\tau}\right)^2 = f(r_0) - f(r). \quad (\text{C2})$$

In four and five dimensions these equations have simple solutions. In five dimensions the solutions are

$$t = \sqrt{f(r_0)}\tau + \frac{\mu}{2} \ln \left| \frac{\tau + \sqrt{f(r_0)}r_0^2/\mu}{\tau - \sqrt{f(r_0)}r_0^2/\mu} \right|, \quad r^2 = r_0^2 - \left(\frac{\mu}{r_0}\right)^2 \tau^2. \quad (\text{C3})$$

Then, performing a coordinate transformation $(t, r) \rightarrow (\tau, r_0)$ the line element becomes

$$ds^2 = -d\tau^2 + \frac{\left(r_0^2 + \left(\frac{\mu}{r_0}\right)^2 \tau^2\right)^2}{r_0^2 - \left(\frac{\mu}{r_0}\right)^2 \tau^2} \frac{dr_0^2}{r_0^2 f(r_0)} + \left(r_0^2 - \left(\frac{\mu}{r_0}\right)^2 \tau^2\right) d\Omega_3. \quad (\text{C4})$$

This coordinate system encodes a space-time slicing with zero shift and constant (unit) lapse (*i.e.* of type (3.1) with $\alpha = 1, \beta^a = 0$) for *all* times. To compare it with a numerical evolution we must have the initial data for the spatial metric written in a conformally flat form. Taking the initial hyper-surface to be $\tau = 0$ we see that this is achieved by a coordinate transformation $r_0 \rightarrow R$ with

$$\frac{dR}{R} = \frac{dr_0}{\sqrt{f(r_0)}r_0} \Rightarrow r_0(R) = R \left(1 + \frac{\mu^2}{4R^2}\right). \quad (\text{C5})$$

This actually coincides with the standard coordinate transformation from Schwarzschild to isotropic coordinates in five dimensions. The line element finally reads (4.8). At the initial hyper-surface $\tau = 0$,

$$ds_{\tau=0}^2 = \left(\frac{r_0(R)}{R}\right)^2 (dR^2 + R^2 d\Omega_3) = \left(\frac{r_0(\sqrt{\rho^2 + z^2})}{\sqrt{\rho^2 + z^2}}\right)^2 (dz^2 + d\rho^2 + \rho^2 d\theta^2 + \rho^2 \sin^2 \theta d\Omega_1), \quad (\text{C6})$$

where we have used the metric on the 3-sphere in the form

$$d\Omega_3 = d\tilde{\theta} + \sin^2 \tilde{\theta} (d\theta^2 + \sin^2 \theta d\Omega_1), \quad (\text{C7})$$

and performed the coordinate transformation $(R, \tilde{\theta}) \rightarrow (\rho, z)$ defined as

$$\rho = R \sin \tilde{\theta}, \quad z = R \cos \tilde{\theta}. \quad (\text{C8})$$

Using (3.12) we get

$$ds_{\tau=0}^2 = \left(\frac{r_0(\sqrt{x^2 + y^2 + z^2})}{\sqrt{x^2 + y^2 + z^2}}\right)^2 (dx^2 + dy^2 + dz^2 + y^2 d\Omega_1). \quad (\text{C9})$$

Thus the coordinate transformation from the spherical coordinates used in (4.8), $(R, \tilde{\theta}, \theta)$, to the ‘‘incomplete’’ Cartesian coordinates used in the numerical evolution (x, y, z) is

$$x = R \sin \tilde{\theta} \cos \theta, \quad y = R \sin \tilde{\theta} \sin \theta, \quad z = R \cos \tilde{\theta}, \quad (\text{C10})$$

which resembles the usual coordinate transformation from spherical polar coordinates to Cartesian coordinates in \mathbb{R}^3 ; but note that $\hat{\theta}$ and θ are *both* polar angles with range $[0, \pi]$, which is the manifestation of the Cartesian coordinates “incompleteness”.

The coordinate change (C10) brings the five dimensional Tangherlini metric in geodesic slicing to a conformally flat form at $\tau = 0$. This matches the initial data for the numerical evolution. One may ask, however, if the coordinate transformation *evolves*, in order to compare the analytic form with the numerical evolution. This cannot be the case, since the existence of τ -dependent terms in the coordinate transformation would imply a drift away from geodesic slicing. We are thus guaranteed that the coordinate transformation (C10) is valid for *all* values of τ . Then, we can predict the value of the metric components that should be obtained from the numerical evolution; say γ_{xx} should be, at time τ

$$\gamma_{xx}(\tau, x, y, z) = \frac{x^2 g_{RR}(\tau, R)}{R^2} + \frac{x^2 z^2 g_{\hat{\theta}\hat{\theta}}(\tau, R)}{R^4(x^2 + y^2)} + \frac{y^2 g_{\theta\theta}(\tau, R)}{(x^2 + y^2)^2}, \quad (\text{C11})$$

where $R^2 = x^2 + y^2 + z^2$ and $g_{RR}(\tau, R)$, $g_{\hat{\theta}\hat{\theta}}(\tau, R)$, $g_{\theta\theta}(\tau, R)$ are readily obtained from (4.8) with (C7) and (C10). The result for $\tilde{\gamma}_{xx}$ along the x -axis is plotted in Fig. 4 for various values of τ .

For $D \geq 6$ the situation is more involved because equations (C2) can no longer be integrated straightforwardly, but require a numerical treatment. First one notices that the coordinate transformation $(t, r) \rightarrow (\tau, r_0)$, with initial conditions $t(\tau = 0) = 0$ and $r(\tau = 0) = r_0$, brings the D dimensional Tangherlini metric to the form

$$ds^2 = -d\tau^2 + \left(\frac{\partial r(\tau, r_0)}{\partial r_0} \right)^2 \frac{dr_0^2}{f(r_0)} + r^2(\tau, r_0) d\Omega_{D-2}. \quad (\text{C12})$$

Then, from the initial conditions, it follows that the coordinate transformation to isotropic coordinates at $\tau = 0$ is

$$\frac{dR}{R} = \frac{dr_0}{\sqrt{f(r_0)}r_0} \stackrel{D \geq 6}{\Rightarrow} r_0(R) = \frac{R}{\mu} \left(1 + \frac{\mu^3}{4R^3} \right)^{2/3}. \quad (\text{C13})$$

Writing the metric on the $(D - 2)$ -sphere as in (C7) (replacing $d\Omega_1 \rightarrow d\Omega_{D-4}$), one concludes that the transformation to “incomplete” Cartesian coordinates is still (C10). Thus (C11) is still valid, which reduces to, along the x -axis ($R = x$):

$$\gamma_{xx}(\tau, x, 0, 0) = g_{RR}(\tau, x) = \frac{r_0(x)^2}{x^2} \left(\frac{\partial r(\tau, r_0)}{\partial r_0} \right)_{r_0=r_0(x)}^2. \quad (\text{C14})$$

This expression is valid for any D . For $D = 6$, $r_0(x)$ is explicitly given by (C13). The derivative in (C14) has to be computed numerically. The result for $\tilde{\gamma}_{xx}$ is plotted, for various values of τ , in Fig. 6.

-
- [1] F. Pretorius, “Evolution of Binary Black Hole Spacetimes,” *Phys. Rev. Lett.* **95** (2005) 121101, [arXiv:gr-qc/0507014](#).
 - [2] M. Campanelli, C. O. Lousto, P. Marronetti, and Y. Zlochower, “Accurate Evolutions of Orbiting Black-Hole Binaries Without Excision,” *Phys. Rev. Lett.* **96** (2006) 111101, [arXiv:gr-qc/0511048](#).
 - [3] J. G. Baker, J. Centrella, D.-I. Choi, M. Koppitz, and J. van Meter, “Gravitational wave extraction from an inspiraling configuration of merging black holes,” *Phys. Rev. Lett.* **96** (2006) 111102, [arXiv:gr-qc/0511103](#).

- [4] J. M. Maldacena, “The large N limit of superconformal field theories and supergravity,” *Adv. Theor. Math. Phys.* **2** (1998) 231–252, [arXiv:hep-th/9711200](#).
- [5] D. T. Son and A. O. Starinets, “Viscosity, Black Holes, and Quantum Field Theory,” *Ann. Rev. Nucl. Part. Sci.* **57** (2007) 95–118, [arXiv:0704.0240 \[hep-th\]](#).
- [6] D. Mateos, “String Theory and Quantum Chromodynamics,” *Class. Quant. Grav.* **24** (2007) S713–S740, [arXiv:0709.1523 \[hep-th\]](#).
- [7] S. A. Hartnoll, “Lectures on holographic methods for condensed matter physics,” *Class. Quant. Grav.* **26** (2009) 224002, [arXiv:0903.3246 \[hep-th\]](#).
- [8] A. J. Amsel, D. Marolf, and A. Virmani, “Collisions with Black Holes and Deconfined Plasmas,” *JHEP* **04** (2008) 025, [arXiv:0712.2221 \[hep-th\]](#).
- [9] S. S. Gubser, S. S. Pufu, and A. Yarom, “Entropy production in collisions of gravitational shock waves and of heavy ions,” *Phys. Rev.* **D78** (2008) 066014, [arXiv:0805.1551 \[hep-th\]](#).
- [10] F. Pretorius and M. W. Choptuik, “Gravitational collapse in 2+1 dimensional AdS spacetime,” *Phys. Rev.* **D62** (2000) 124012, [arXiv:gr-qc/0007008](#).
- [11] H. Witek, V. Cardoso, L. Gualtieri, C. Herdeiro, A. Nerozzi, U. Sperhake, and M. Zilhão, “Black holes in a box: towards the numerical evolution of black holes in AdS,” [arXiv:1004.4633 \[hep-th\]](#).
- [12] I. Antoniadis, “A Possible new dimension at a few TeV,” *Phys. Lett.* **B246** (1990) 377–384.
- [13] N. Arkani-Hamed, S. Dimopoulos, and G. R. Dvali, “The hierarchy problem and new dimensions at a millimeter,” *Phys. Lett.* **B429** (1998) 263–272, [arXiv:hep-ph/9803315](#).
- [14] I. Antoniadis, N. Arkani-Hamed, S. Dimopoulos, and G. R. Dvali, “New dimensions at a millimeter to a Fermi and superstrings at a TeV,” *Phys. Lett.* **B436** (1998) 257–263, [arXiv:hep-ph/9804398](#).
- [15] L. Randall and R. Sundrum, “A large mass hierarchy from a small extra dimension,” *Phys. Rev. Lett.* **83** (1999) 3370–3373, [arXiv:hep-ph/9905221](#).
- [16] L. Randall and R. Sundrum, “An alternative to compactification,” *Phys. Rev. Lett.* **83** (1999) 4690–4693, [arXiv:hep-th/9906064](#).
- [17] P. C. Argyres, S. Dimopoulos, and J. March-Russell, “Black holes and sub-millimeter dimensions,” *Phys. Lett.* **B441** (1998) 96–104, [arXiv:hep-th/9808138](#).
- [18] T. Banks and W. Fischler, “A model for high energy scattering in quantum gravity,” [arXiv:hep-th/9906038](#).
- [19] S. B. Giddings and S. D. Thomas, “High energy colliders as black hole factories: The end of short distance physics,” *Phys. Rev.* **D65** (2002) 056010, [arXiv:hep-ph/0106219](#).
- [20] S. Dimopoulos and G. L. Landsberg, “Black Holes at the LHC,” *Phys. Rev. Lett.* **87** (2001) 161602, [arXiv:hep-ph/0106295](#).
- [21] E.-J. Ahn, M. Cavaglia, and A. V. Olinto, “Brane factories,” *Phys. Lett.* **B551** (2003) 1–6, [arXiv:hep-th/0201042](#).
- [22] A. Chamblin, F. Cooper, and G. C. Nayak, “SUSY production from TeV scale blackhole at LHC,” *Phys. Rev.* **D70** (2004) 075018, [arXiv:hep-ph/0405054](#).
- [23] J. L. Feng and A. D. Shapere, “Black hole production by cosmic rays,” *Phys. Rev. Lett.* **88** (2002) 021303, [arXiv:hep-ph/0109106](#).
- [24] E.-J. Ahn, M. Ave, M. Cavaglia, and A. V. Olinto, “TeV black hole fragmentation and detectability in extensive air-showers,” *Phys. Rev.* **D68** (2003) 043004, [arXiv:hep-ph/0306008](#).
- [25] V. Cardoso, M. C. Espirito Santo, M. Paulos, M. Pimenta, and B. Tome, “Microscopic black hole detection in UHECR: The double bang signature,” *Astropart. Phys.* **22** (2005) 399–407, [arXiv:hep-ph/0405056](#).
- [26] M. Banados, J. Silk, and S. M. West, “Kerr Black Holes as Particle Accelerators to Arbitrarily High Energy,” *Phys. Rev. Lett.* **103** (2009) 111102, [arXiv:0909.0169 \[hep-ph\]](#).
- [27] E. Berti, V. Cardoso, L. Gualtieri, F. Pretorius, and U. Sperhake, “Comment on ‘Kerr Black Holes as Particle Accelerators to Arbitrarily High Energy’,” *Phys. Rev. Lett.* **103** (2009) 239001, [arXiv:0911.2243 \[gr-qc\]](#).
- [28] T. Jacobson and T. P. Sotiriou, “Spinning Black Holes as Particle Accelerators,” [arXiv:0911.3363 \[gr-qc\]](#).
- [29] M. Cavaglia, “Black hole and brane production in TeV gravity: A review,” *Int. J. Mod. Phys.* **A18** (2003) 1843–1882, [arXiv:hep-ph/0210296](#).
- [30] P. Kanti, “Black holes in theories with large extra dimensions: A Review,” *Int. J. Mod. Phys.* **A19** (2004) 4899–4951, [arXiv:hep-ph/0402168](#).
- [31] P. Kanti, “Black Holes at the LHC,” *Lect. Notes Phys.* **769** (2009) 387–423,

- arXiv:0802.2218 [hep-th].
- [32] S. N. Solodukhin, “Classical and quantum cross-section for black hole production in particle collisions,” *Phys. Lett.* **B533** (2002) 153–161, arXiv:hep-ph/0201248.
 - [33] S. D. H. Hsu, “Quantum production of black holes,” *Phys. Lett.* **B555** (2003) 92–98, arXiv:hep-ph/0203154.
 - [34] J. A. Frost *et al.*, “Phenomenology of Production and Decay of Spinning Extra- Dimensional Black Holes at Hadron Colliders,” *JHEP* **10** (2009) 014, arXiv:0904.0979 [hep-ph].
 - [35] M. Cavaglia, R. Godang, L. Cremaldi, and D. Summers, “Catfish: A Monte Carlo simulator for black holes at the LHC,” *Comput. Phys. Commun.* **177** (2007) 506–517, arXiv:hep-ph/0609001.
 - [36] D.-C. Dai *et al.*, “BlackMax: A black-hole event generator with rotation, recoil, split branes and brane tension,” *Phys. Rev.* **D77** (2008) 076007, arXiv:0711.3012 [hep-ph].
 - [37] D.-C. Dai *et al.*, “Manual of BlackMax, a black-hole event generator with rotation, recoil, split branes, and brane tension,” arXiv:0902.3577 [hep-ph].
 - [38] D. M. Eardley and S. B. Giddings, “Classical black hole production in high-energy collisions,” *Phys. Rev.* **D66** (2002) 044011, arXiv:gr-qc/0201034.
 - [39] E. Kohlprath and G. Veneziano, “Black holes from high-energy beam-beam collisions,” *JHEP* **06** (2002) 057, arXiv:gr-qc/0203093.
 - [40] H. Yoshino and Y. Nambu, “High-energy head-on collisions of particles and hoop conjecture,” *Phys. Rev.* **D66** (2002) 065004, arXiv:gr-qc/0204060.
 - [41] H. Yoshino and Y. Nambu, “Black hole formation in the grazing collision of high- energy particles,” *Phys. Rev.* **D67** (2003) 024009, arXiv:gr-qc/0209003.
 - [42] P. D. D’Eath and P. N. Payne, “Gravitational radiation in high speed black hole collisions. 1. Perturbation treatment of the axisymmetric speed of light collision,” *Phys. Rev.* **D46** (1992) 658–674.
 - [43] P. D. D’Eath and P. N. Payne, “Gravitational radiation in high speed black hole collisions. 2. Reduction to two independent variables and calculation of the second order news function,” *Phys. Rev.* **D46** (1992) 675–693.
 - [44] P. D. D’Eath and P. N. Payne, “Gravitational radiation in high speed black hole collisions. 3. Results and conclusions,” *Phys. Rev.* **D46** (1992) 694–701.
 - [45] V. Cardoso and J. P. S. Lemos, “Gravitational radiation from collisions at the speed of light: A massless particle falling into a Schwarzschild black hole,” *Phys. Lett.* **B538** (2002) 1–5, arXiv:gr-qc/0202019.
 - [46] E. Berti, M. Cavaglia, and L. Gualtieri, “Gravitational energy loss in high energy particle collisions: Ultrarelativistic plunge into a multidimensional black hole,” *Phys. Rev.* **D69** (2004) 124011, arXiv:hep-th/0309203.
 - [47] V. Cardoso, E. Berti, and M. Cavaglia, “What we (don’t) know about black hole formation in high-energy collisions,” *Class. Quant. Grav.* **22** (2005) L61–R84, arXiv:hep-ph/0505125.
 - [48] U. Sperhake, V. Cardoso, F. Pretorius, E. Berti, and J. A. Gonzalez, “The high-energy collision of two black holes,” *Phys. Rev. Lett.* **101** (2008) 161101, arXiv:0806.1738 [gr-qc].
 - [49] M. Shibata, H. Okawa, and T. Yamamoto, “High-velocity collision of two black holes,” *Phys. Rev.* **D78** (2008) 101501, arXiv:0810.4735 [gr-qc].
 - [50] U. Sperhake *et al.*, “Cross section, final spin and zoom-whirl behavior in high- energy black hole collisions,” *Phys. Rev. Lett.* **103** (2009) 131102, arXiv:0907.1252 [gr-qc].
 - [51] R. Emparan and H. S. Reall, “Black Holes in Higher Dimensions,” *Living Rev. Rel.* **11** (2008) 6, arXiv:0801.3471 [hep-th].
 - [52] R. Emparan and R. C. Myers, “Instability of ultra-spinning black holes,” *JHEP* **09** (2003) 025, arXiv:hep-th/0308056.
 - [53] O. J. C. Dias, P. Figueras, R. Monteiro, J. E. Santos, and R. Emparan, “Instability and new phases of higher-dimensional rotating black holes,” arXiv:0907.2248 [hep-th].
 - [54] M. Shibata and H. Yoshino, “Nonaxisymmetric instability of rapidly rotating black hole in five dimensions,” arXiv:0912.3606 [gr-qc].
 - [55] V. Cardoso and L. Gualtieri, “Equilibrium configurations of fluids and their stability in higher dimensions,” *Class. Quant. Grav.* **23** (2006) 7151–7198, arXiv:hep-th/0610004.
 - [56] V. Cardoso and O. J. C. Dias, “Bifurcation of Plasma Balls and Black Holes to Lobed Configurations,” *JHEP* **04** (2009) 125, arXiv:0902.3560 [hep-th].
 - [57] V. Cardoso, O. J. C. Dias, and J. V. Rocha, “Phase diagram for non-axisymmetric plasma balls,” arXiv:0910.0020 [hep-th].

- [58] R. Gregory and R. Laflamme, “Black strings and p-branes are unstable,” *Phys. Rev. Lett.* **70** (1993) 2837–2840, [arXiv:hep-th/9301052](#).
- [59] M. Choptuik, L. Lehner, I. Olabarrieta, R. Petryk, F. Pretorius, and H. Villegas, “Towards the final fate of an unstable black string,” *Phys. Rev.* **D68** (2003) 044001, [arXiv:gr-qc/0304085](#).
- [60] E. Sorkin and M. W. Choptuik, “Generalized harmonic formulation in spherical symmetry,” [arXiv:0908.2500 \[gr-qc\]](#).
- [61] E. Sorkin, “An axisymmetric generalized harmonic evolution code,” [arXiv:0911.2011 \[gr-qc\]](#).
- [62] M. Headrick, S. Kitchen, and T. Wiseman, “A new approach to static numerical relativity, and its application to Kaluza-Klein black holes,” [arXiv:0905.1822 \[gr-qc\]](#).
- [63] M. Alcubierre, S. Brandt, B. Brügmann, D. Holz, E. Seidel, R. Takahashi, and J. Thornburg, “Symmetry without Symmetry: Numerical Simulation of Axisymmetric Systems using Cartesian Grids,” *Int. J. Mod. Phys.* **D10** (2001) 273–290, [arXiv:gr-qc/9908012](#).
- [64] H. Yoshino and M. Shibata, “Higher-dimensional numerical relativity: Formulation and code tests,” *Phys. Rev.* **D80** (2009) 084025, [arXiv:0907.2760 \[gr-qc\]](#).
- [65] K.-i. Nakao, H. Abe, H. Yoshino, and M. Shibata, “Maximal slicing of D-dimensional spherically-symmetric vacuum spacetime,” *Phys. Rev.* **D80** (2009) 084028, [arXiv:0908.0799 \[gr-qc\]](#).
- [66] M. Shibata and T. Nakamura, “Evolution of three-dimensional gravitational waves: Harmonic slicing case,” *Phys. Rev.* **D52** (1995) 5428–5444.
- [67] T. W. Baumgarte and S. L. Shapiro, “On the numerical integration of Einstein’s field equations,” *Phys. Rev.* **D59** (1999) 024007, [arXiv:gr-qc/9810065](#).
- [68] U. Sperhake, “Binary black-hole evolutions of excision and puncture data,” *Phys. Rev.* **D76** (2007) 104015, [arXiv:gr-qc/0606079](#).
- [69] F. R. Tangherlini, “Schwarzschild field in n dimensions and the dimensionality of space problem,” *Nuovo Cim.* **27** (1963) 636–651.
- [70] R. P. Geroch, “A Method for generating solutions of Einstein’s equations,” *J. Math. Phys.* **12** (1971) 918–924.
- [71] K. R. P. Sjoдин, U. Sperhake, and J. A. Vickers, “Dynamic cosmic strings. I,” *Phys. Rev.* **D63** (2001) 024011, [arXiv:gr-qc/0002096](#).
- [72] U. Sperhake, K. R. P. Sjoдин, and J. A. Vickers, “Dynamic cosmic strings. II: Numerical evolution of excited cosmic strings,” *Phys. Rev.* **D63** (2001) 024012, [arXiv:gr-qc/0003114](#).
- [73] M. W. Choptuik, E. W. Hirschmann, S. L. Liebling, and F. Pretorius, “An Axisymmetric Gravitational Collapse Code,” *Class. Quant. Grav.* **20** (2003) 1857–1878, [arXiv:gr-qc/0301006](#).
- [74] C. C. Chiang, S. C. Lee, and G. Marmo, “Curvature Tensor For Kaluza-Klein Theories With Homogeneous Fibers,” *Phys. Rev.* **D32** (1985) 1364.
- [75] Y. M. Cho, “Dimensional Reduction by Isometry,” *Phys. Lett* **186B** (1987) 38.
- [76] Y. M. Cho and D. S. Kim, “Higher Dimensional Unification By Isometry,” *J. Math. Phys.* **30** (1989) 1570–1578.
- [77] R. Arnowitt, S. Deser, and C. W. Misner, “The dynamics of general relativity,” [arXiv:gr-qc/0405109](#).
- [78] J. W. York, Jr., “Kinematics and dynamics of general relativity,” in *Sources of Gravitational Radiation*, L. L. Smarr, ed., pp. 83–126. 1979.
- [79] E.ourgoulhon, “3+1 Formalism and Bases of Numerical Relativity,” [arXiv:gr-qc/0703035](#).
- [80] M. Alcubierre, *Introduction to 3+1 numerical relativity*. International series of monographs on physics. Oxford Univ. Press, Oxford, 2008.
- [81] H. Yoshino, T. Shiromizu, and M. Shibata, “The close limit analysis for head-on collision of two black holes in higher dimensions: Brill-Lindquist initial data,” *Phys. Rev.* **D72** (2005) 084020, [arXiv:gr-qc/0508063](#).
- [82] H. Yoshino, T. Shiromizu, and M. Shibata, “Close-slow analysis for head-on collision of two black holes in higher dimensions: Bowen-York initial data,” *Phys. Rev.* **D74** (2006) 124022, [arXiv:gr-qc/0610110](#).
- [83] S. Brandt and B. Brügmann, “Black hole punctures as initial data for general relativity,” *Phys. Rev. Lett.* **78** (1997) 3606–3609, [arXiv:gr-qc/9703066](#).
- [84] “Cactus Computational Toolkit.” <http://www.cactuscode.org/>.
- [85] E. Schnetter, S. H. Hawley, and I. Hawke, “Evolutions in 3D numerical relativity using fixed mesh refinement,” *Class. Quant. Grav.* **21** (2004) 1465–1488, [arXiv:gr-qc/0310042](#).
- [86] “Mesh refinement with Carpet.” <http://www.carpetcode.org/>.

- [87] M. Ansorg, B. Bruegmann, and W. Tichy, “A single-domain spectral method for black hole puncture data,” *Phys. Rev.* **D70** (2004) 064011, [arXiv:gr-qc/0404056](#).
- [88] J. Thornburg, “Finding apparent horizons in numerical relativity,” *Phys. Rev.* **D54** (1996) 4899–4918, [arXiv:gr-qc/9508014](#).
- [89] J. Thornburg, “A Fast Apparent-Horizon Finder for 3-Dimensional Cartesian Grids in Numerical Relativity,” *Class. Quant. Grav.* **21** (2004) 743–766, [arXiv:gr-qc/0306056](#).
- [90] E. Seidel, “Gravitational radiation from even parity perturbations of stellar collapse: Mathematical formalism and numerical methods,” *Phys. Rev.* **D42** (1990) 1884–1907.
- [91] M. Gabler, U. Sperhake, and N. Andersson, “Non-linear radial oscillations of neutron stars,” *Phys. Rev.* **D80** (2009) 064012, [arXiv:0906.3088 \[gr-qc\]](#).